Doctor of Philosophy

Serial analysis of *ESR1* and *PIK3CA* mutations in cell-free DNA from hormone receptor-positive, HER2-negative metastatic breast cancer during palliative endocrine therapy

The Graduate School
of the University of Ulsan

Department of Medicine
Soo Yeon Baek

Serial analysis of *ESR1* and *PIK3CA* mutations in cell-free DNA from hormone receptor-positive, HER2-negative metastatic breast cancer during palliative endocrine therapy

Supervisor: Sae Byul Lee

A Dissertation

Submitted to

the Graduate School of the University of Ulsan

In partial Fulfillment of the Requirements

for the Degree of

Doctor of Philosophy

by

Soo Yeon Baek

Department of Medicine

Ulsan, Korea

August 2024

Serial analysis of *ESR1* and *PIK3CA* mutations in cell-free DNA from hormone receptor-positive, HER2-negative metastatic breast cancer during palliative endocrine therapy

This certifies that the dissertation
of Soo Yeon Baek is approved.

Jae Ho Jeong

Committee Chair Dr.

Sung Gwe Ahn

Committee Member Dr.

Jisun Kim

Committee Member Dr.

Tae-Kyung Yoo

Committee Member Dr.

Sae Byul Lee

Committee Member Dr.

Department of Medicine

Ulsan, Korea

August 2024

Abstract

Background: Activating mutations in estrogen receptor 1 (*ESR1*) and phosphatidylinositol-4,5-bisphosphate 3-kinase catalytic subunit alpha (*PIK3CA*) genes are known mechanisms of endocrine resistance. A recent analysis supported the benefit of early intervention when the presence of *ESR1* mutations is detected in the blood (b*ESR1*) before clinical progression. Herein, we aimed to investigate *ESR1* and *PIK3CA* mutations detected in cell-free DNA (cfDNA) from patients with hormone receptor-positive, human epidermal growth factor receptor 2-negative metastatic breast cancer and their impact on progression-free survival (PFS).

Methods: A total of 25 patients who underwent first-line palliative endocrine therapy (ETx) were included in this study from a prospective cohort. Seven *ESR1* hotspot mutations in the ligand-binding domain were tested in cfDNA using a droplet digital polymerase chain reaction assay, and eleven *PIK3CA* hotspot mutations were tested using an amplicon-based targeted next-generation sequencing method for both tumors and cfDNA. PFS analyses were performed using the Kaplan–Meier method and compared using the log-rank test.

Results: We examined 268 cfDNA samples collected from 25 patients every three to six months. b*ESR1* was observed in 64.0% (16/25) of the patients, with D538G being the most common mutation and 68.8% polyclonal. Among the 50.0% of the patients with b*ESR1* mutations with clinical progression, b*ESR1* was detected in four before clinical progression, and four were diagnosed with clinical progression concurrently or after. While b*ESR1* mutation did not affect overall PFS, patients with b*ESR1* detected within 6 months of first-line ETx (18.8%) displayed worse outcomes (median PFS 5.5 vs. 53.6 months). Notably, patients with b*ESR1* cleared in the subsequent cfDNA analysis (81.3%) had better outcomes (median PFS

53.6 vs. 42.4 months). Furthermore, *PIK3CA* mutations in cfDNA were detected in 68.2% (15/22) of the patients at the time of distant metastasis diagnosis, of whom 53.3% (8/15) had b*ESR1*. While the presence of *PIK3CA* mutations in the primary tumor tissue did not affect disease-free survival or PFS, patients with blood *PIK3CA* mutations displayed significantly worse PFS ($p = 0.024$).

Conclusions: A substantial number of b*ESR1* and *PIK3CA* mutations were detected in serial plasma samples. Although it was a small-sized analysis to accurately assess statistical significance, we observed worse outcomes in patients with early detection within 6 months and sustained b*ESR1* expression during palliative ETx. *PIK3CA* mutations in cfDNA are prognostic factors, supporting the benefits of combined targeted therapies.

Contents

Abstract ..... **i**

List of Tables and Figures ..... **iv**

1. Introduction **1**

1.1 Estrogen receptor-positive breast cancer 1

1.2 Estrogen receptor 1 mutation 1

1.3 *PIK3CA* mutation 2

1.4 Circulating tumor DNA 3

1.5 ctDNA monitoring 3

2. Purpose **4**

3. Methods **5**

3.1 Patients 5

3.2 Sample collection and processing 7

3.3 Cell-free DNA extraction 7

3.4 Detection of ctDNA 7

3.5 Droplet digital PCR 8

3.6 Amplicon-based targeted NGS 9

3.7 Statistical analysis 10

4. Results **11**

4.1 cfDNA samples 11

4.2 Characteristics of the patients 11

4.3 Treatment 15

4.4 *ESR1* mutation 17

4.5 *PIK3CA* mutation 51

4.6 *ESR1* and *PIK3CA* mutations 57

5. Discussion **61**

6. References **68**

Korean Abstract **76**

List of Tables and Figures

Table 1. Patients characteristics (n = 25) ····· 12

Figure 1. Flow diagram of patient selection criteria ····· 6

Figure 2. Swimmer plot presenting *ESR1* mutation status and clinical information of individual patients after palliative first-line endocrine therapy ····· 16

Figure 3. *ESR1* D538G mutation droplet digital polymerase chain reaction result and plot for the DNAM043 patient ····· 17

Figure 4. *ESR1* D538G mutation droplet digital polymerase chain reaction result and plot for the DNAM009 patient ····· 18

Figure 5. *ESR1* D538G mutation droplet digital polymerase chain reaction result and plot for the DNAM011 patient ····· 19

Figure 6. *ESR1* D538G mutation droplet digital polymerase chain reaction result and plot for the DNAM014 patient ····· 20

Figure 7. *ESR1* D538G mutation droplet digital polymerase chain reaction result and plot for the DNAM017 patient ····· 21

Figure 8. *ESR1* D538G mutation droplet digital polymerase chain reaction result and plot for the DNAM024 patient ····· 22

Figure 9. *ESR1* D538G mutation droplet digital polymerase chain reaction result and plot for the M0005 patient ····· 23

Figure 10. *ESR1* D538G mutation droplet digital polymerase chain reaction result and plot for the M0008 patient ····· 24

Figure 11. *ESR1* D538G mutation droplet digital polymerase chain reaction result and plot for the AMCM007 patient ····· 25

Figure 12. *ESR1* S643P mutation droplet digital polymerase chain reaction result and plot for the AMCM031 patient ····· 26

Figure 13. *ESR1* S643P mutation droplet digital polymerase chain reaction result and plot for the DNAM043 patient ····· 27

Figure 14. *ESR1* S643P mutation droplet digital polymerase chain reaction result and plot for the DNAM009 patient ····· 28

Figure 15. *ESR1* S643P mutation droplet digital polymerase chain reaction result and plot for the DNAM011 patient ····· 29

Figure 16. *ESR1* S643P mutation droplet digital polymerase chain reaction result and plot for the DNAM014 patient ····· 30

Figure 17. *ESR1* S643P mutation droplet digital polymerase chain reaction result and plot for the DNAM017 patient ····· 31

Figure 18. *ESR1* S643P mutation droplet digital polymerase chain reaction result and plot for the DNAM024 patient ····· 32

Figure 19. *ESR1* S643P mutation droplet digital polymerase chain reaction result and plot for the DNAM027 patient ····· 33

Figure 20. *ESR1* Y537N mutation droplet digital polymerase chain reaction result and plot for the AMCM037 patient ····· 34

Figure 21. *ESR1* Y537N mutation droplet digital polymerase chain reaction result and plot for the DNAM043 patient ····· 34

Figure 22. *ESR1* Y537N mutation droplet digital polymerase chain reaction result and plot for the DNAM002 patient ····· 35

Figure 23. *ESR1* Y537N mutation droplet digital polymerase chain reaction result and plot for the DNAM011 patient ····· 35

Figure 24. *ESR1* Y537N mutation droplet digital polymerase chain reaction result and plot for the DNAM014 patient ····· 36

Figure 25. *ESR1* Y537C mutation droplet digital polymerase chain reaction result and plot for the DNAM033 patient ····· 36

Figure 26. *ESR1* Y537C mutation droplet digital polymerase chain reaction result and plot for the AMCM031 patient ····· 37

Figure 27. *ESR1* Y537C mutation droplet digital polymerase chain reaction result and plot for the AMCM037 patient ····· 38

Figure 28. *ESR1* Y537C mutation droplet digital polymerase chain reaction result and plot for the DANM043 patient ····· 39

Figure 29. *ESR1* Y537C mutation droplet digital polymerase chain reaction result and plot for the DNAM009 patient ····· 40

Figure 30. *ESR1* Y537C mutation droplet digital polymerase chain reaction result and plot for the DNAM014 patient ····· 41

Figure 31. *ESR1* Y537C mutation droplet digital polymerase chain reaction result and plot for the DNAM038 patient ····· 41

Figure 32. *ESR1* Y537C mutation droplet digital polymerase chain reaction result and plot for the M0005 patient ····· 42

Figure 33. *ESR1* Y537S mutation droplet digital polymerase chain reaction result and plot for the AMCM027 patient ····· 42

Figure 34. *ESR1* Y537S mutation droplet digital polymerase chain reaction result and plot for the DNAM027 patient ····· 43

Figure 35. *ESR1* E380Q mutation droplet digital polymerase chain reaction result and plot for the DNAM033 patient ····· 43

Figure 36. Swimmer plot showing the *ESR1* mutation status and clinical information of individual patients after initiation of endocrine therapy ····· 45

Figure 37. Kaplan–Meier curves of progression-free survival according to *ESR1* mutation status ····· 46

Figure 38A. Kaplan–Meier curves of progression-free survival according to *ESR1* mutation detection time ····· 47

Figure 38B. Kaplan–Meier curves of progression-free survival according to *ESR1* clearance ····· 48

Figure 38C. Kaplan–Meier curves of progression-free survival according to polyclonality of *ESR1* mutations ····· 49

Figure 39. Kaplan–Meier curves of progression-free survival for disease-progressed patients according to *ESR1* status ····· 50

Figure 40. *PIK3CA* mutation status ····· 52

Figure 41A. Kaplan–Meier curves of progression-free survival according to *PIK3CA* mutations in plasma ····· 53

Figure 41B. Kaplan–Meier curves of progression-free survival according to *PIK3CA* mutations in primary tumor tissue ····· 54

Figure 41C. Kaplan–Meier curves of disease-free survival according to *PIK3CA* mutations in primary tumor tissue ····· 55

Figure 41D. Kaplan–Meier curves of progression-free survival according to *PIK3CA* mutations in metastatic tumor tissue ····· 56

Figure 42. Kaplan–Meier curves of progression-free survival according to progression-free survival according to co-occurrence of *ESR1* and *PIK3CA* mutation in plasma ····· 57

Figure 43. ctDNA trajectories in patient DNAM033 ····· 58

Figure 44. ctDNA trajectories in patient DNAM043 ····· 59

Figure 45. ctDNA trajectories in patient DNAM014 ····· 59

Figure 46. ctDNA trajectories in patient DNAM027 ····· 60

1. Introduction

1.1 Estrogen receptor-positive breast cancer

Approximately 80% of the breast cancers express estrogen receptor (ER) (1). Endocrine therapy (ETx), which targets the ER, is the standard adjuvant treatment for this type of tumor. Several classes of endocrine agents with different mechanisms of action have been used to treat ER-positive breast cancer. All of these treatments block ER function and signaling. Selective ER modulators, such as tamoxifen, have anti-estrogenic activity mediated by competitive inhibition of estrogen-ER binding (2). Aromatase inhibitors (AI) inhibit the conversion of androgens into estrogens (3). Selective estrogen receptor degraders (SERD) such as fulvestrant bind to ER and downregulate it through ER degradation (4). ETx significantly reduces the recurrence and mortality rates of ER-positive breast cancer (5). However, even after receiving these therapies, patients with ER-positive breast cancer have a persistent risk of recurrence for up to 20 years after diagnosis (6). Notably, endocrine resistance remains a major clinical challenge in treating ER-positive breast cancer. Breast cancer acquires endocrine resistance through various mechanisms (7). Mutations in estrogen receptor 1 (*ESR1*) and phosphatidylinositol-4,5-bisphosphate 3-kinase catalytic subunit alpha (*PIK3CA*) mutations are known mechanisms of endocrine resistance in hormone receptor (HR)-positive breast cancer. The presence of these mutations is associated with poor prognosis (8-10).

1.2 Estrogen receptor 1 mutation

ER is a transcription factor that consists of functional domains encoded by *ESR1* (11). *ESR1* mutation confer endocrine resistance by altering the structure and function in the ligand

binding domain of ERα (12). *ESR1* mutations are rare in primary breast cancer but are enriched in metastatic breast cancer, particularly in patients previously exposed to AIs (13, 14). *ESR1* mutations were first reported in 1996 (15), and their clinical significance was discovered later. Several studies have revealed the role of *ESR1* mutations as prognostic biomarkers (9, 10). A study that conducted circulating tumor DNA (ctDNA) analysis of plasma samples from patients in the "Study of Faslodex versus Exemestane with or without Arimidex (SoFEA)" trial showed that patients with *ESR1* mutations had improved progression-free survival (PFS) when treated with fulvestrant compared to those treated with exemestane (16). Fulvestrant is a first-in-class SERD. However, fulvestrant has a low bioavailability and is delivered via intramuscular injections. In addition, a preclinical study reported reduced efficacy of fulvestrant due to a specific type of *ESR1* mutation (17). To overcome this limitation, orally bioavailable SERDs have been developed, and some studies have reported positive results (18, 19). In the EMERALD trial (NCT03778931), elacestrant first demonstrated a significant improvement in PFS in patients with *ESR1* mutations (18).

1.3 *PIK3CA* mutation

The phosphatidylinositol 3-kinase (PI3K) pathway is frequently dysregulated in cancers. This pathway is associated with disease progression and endocrine resistance in breast cancer (20). The *PIK3CA* gene encodes the p110α catalytic subunit of PI3K, mediating cell survival, differentiation, and proliferation (21). *PIK3CA* mutations have been reported in up to 40% of patients with metastatic HR-positive breast cancer (22-25). The prognostic and predictive value of *PIK3A* mutations has also been elucidated (26). *PIK3CA* mutation has emerged as a therapeutic target for HR-positive/human epidermal growth factor receptor 2 (HER2)-negative metastatic breast cancer. Some PI3K inhibitors and isoform-selective PI3K inhibitors have

been developed (27, 28). Some studies have shown synergistic effects of PI3K inhibitors and ETx (29, 30). The PFS benefits of targeted therapy based on *PIK3CA* mutations have been reported in metastatic HR-positive breast cancer (27).

1.4 Circulating tumor DNA

ctDNA analysis from cell-free DNA (cfDNA) has emerged as an important tool for detecting these clinically relevant mutations. In some patients with metastases, it may not be possible to obtain metastatic tissues. Liquid biopsy using ctDNA from cfDNA is a non-invasive method for detecting mutations. ctDNA is present in very low fractions, constituting less than 1% of the total cfDNA, and a highly sensitive method is required to detect it (31). Notably, advances in genomic technology have enabled the identification of rare mutant variants (32). *ESR1* mutations are subclonally acquired in cancers during ETx. ctDNA testing detects approximately 20–40% of *ESR1* mutations in metastatic breast cancer (13, 14, 16) and is recommended as a primary test for *ESR1* mutation detection (33). Polymerase chain reaction (PCR)- and next-generation sequencing (NGS)-based tests of blood are recommended as companion diagnostics to identify *PIK3CA* mutations to administer PI3K inhibitors (34).

1.5 ctDNA monitoring

Evidence for the serial monitoring of ctDNA during treatment is limited. In a clinical trial evaluating the efficacy of inhibitors of cyclin-dependent kinases 4 and 6 (CDK4/6i) in ER-positive breast cancer, short-term reduction in *PIK3CA* ctDNA levels predicted prognosis and treatment response (22). It has also been reported that ctDNA increases during treatment-identified disease progression in a significant proportion of patients before detection in

radiological studies using longitudinal ctDNA analysis (35). These results indicate the utility of measuring serial ctDNA levels during treatment to detect disease progression and rapidly optimize treatment. In a randomized phase III PADA-1 trial (NCT03079011), patients with ER-positive/HER2-negative advanced breast cancer receiving first-line AI and CDK4/6i therapy were recruited and monitored for rising blood *ESR1* (b*ESR1*) mutations (36). Switching ETx after the elevation of the b*ESR1* mutations and before clinical tumor progression significantly improved PFS in these patients. These results demonstrate the clinical benefit of a targeted approach using ctDNA monitoring.

2. Purpose

In this study, we identified *ESR1* and *PIK3CA* mutations in the ctDNA of patients with HR-positive/HER2-negative metastatic breast cancer using droplet digital PCR (ddPCR) assays and amplicon-based targeted NGS with plasma samples collected at multiple time points. We aimed to track *ESR1* mutation changes during palliative treatment and compare mutation detection and the timing of clinical disease progression. We also analyzed the association between *ESR1* and *PIK3CA* mutations and PFS.

3. Methods

3.1 Patients

Patients with recurrent or metastatic breast cancer were identified from a previously established prospective circulating tumor cell and ctDNA cohort in August 2017 at Asan Medical Center, Seoul, Republic of Korea. We identified patients who were enrolled until March 21, 2023. Patients with HR-negative or HER2-positive tumors were excluded. Patients whose HR or HER2 status changed in the metastatic tissue were also excluded. Patients were eligible if primary breast cancer tissue was present at diagnosis, plasma samples were collected at the time of metastasis, and serial blood samples were collected during ETx. Among the patients who received palliative first-line ETx, 25 were included in this study (Figure 1). This study was approved by the Institutional Review Board of the Asan Medical Center (2019-1480). Written informed consent was previously obtained from all patients in the cohort. HR positivity was defined as nuclear staining ≥1% or an Allred score of 3–8 based on the results of immunohistochemistry (IHC) staining for the ER or progesterone receptor. HER2 positivity was defined as 3+ by IHC staining, HER2 gene amplification by fluorescence in situ hybridization (FISH), or silver-enhanced in situ hybridization (SISH). HER2 grade 2+ (equivocal) without FISH or SISH testing was defined as an unknown HER2 status and was excluded. Primary endocrine resistance was defined as relapse during the first two years of adjuvant ETx or progression during the first six months of first-line ETx. Secondary endocrine resistance was defined as disease relapse while on adjuvant ETx but after the first two years, relapse within 12 months of completing adjuvant ETx, or progressive disease ≥6 months after initiating first-line ETx (37). The clinical response to palliative therapy was assessed according to the physician's assessment of the radiological evidence of changes in the burden of disease. The first-line or later lines of treatment were decided by the physician or through consultation with a multidisciplinary

clinic consisting of a breast surgeon, medical oncologist, radiation oncologist, pathologist, radiologist, and nuclear radiologist.

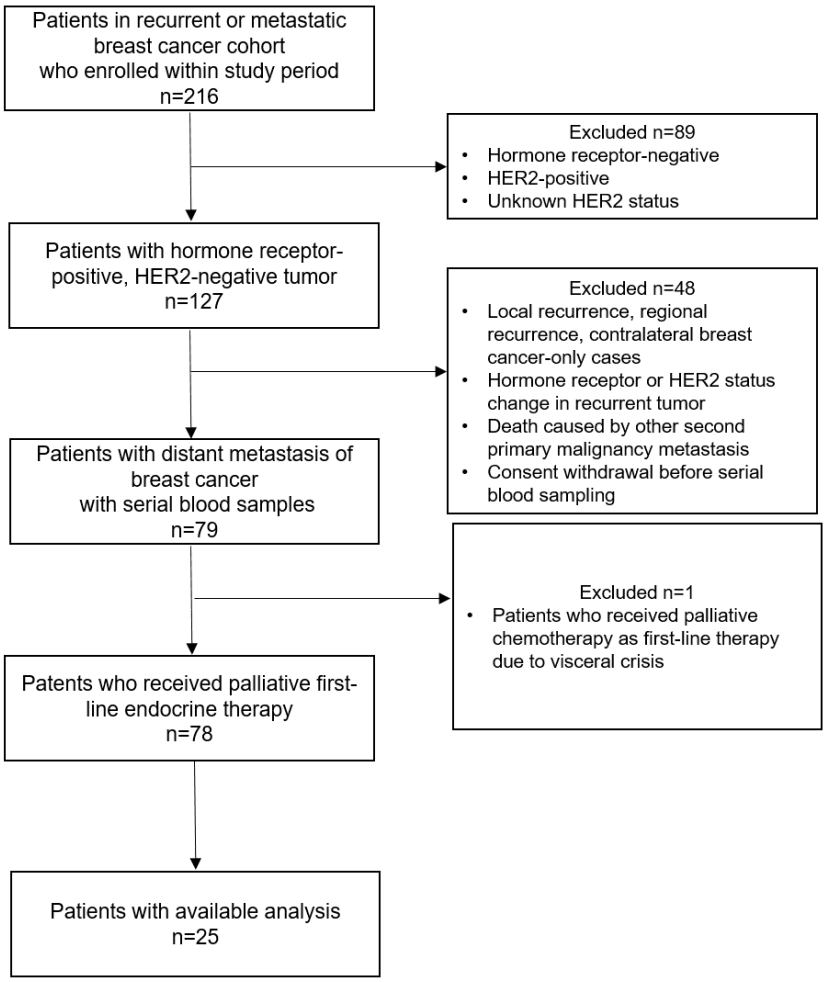

Figure 1. Flow diagram of patient selection criteria

HER2, Human epidermal growth factor receptor 2

3.2 Sample collection and processing

Blood collection was planned at intervals of 3–6 months, according to each patient's hospital visit and blood sampling schedule. Blood samples were collected in EDTA blood collection tubes. The samples were processed within one hour of collection. Plasma was obtained by double centrifugation at 1600 ×g for 10 minutes at 4 ℃ and 3000 ×g for 10 minutes at 4 ℃. The plasma was stored at -80 ℃ prior to cfDNA extraction.

3.3 Cell-free DNA extraction

cfDNA was extracted from 2 mL of plasma. For tumors, DNA was extracted from the microdissected specimens. The extraction was performed using the QIAamp Circulating Nucleic Acid Kit (Qiagen, Hilden, Germany) according to the manufacturer's protocol.

3.4 Detection of ctDNA

ESR1 mutations were defined as seven hotspot mutations (D538G, Y537C, Y537S, Y537N, L536R, S463P, and E380Q) among missense mutations in the ligand-binding domain (Codon 310-547). *ESR1* hotspot mutations in the ligand-binding domain were detected in cfDNA by ddPCR using an *ESR1* mutations detection kit (Genopeaks Co., Ltd., Seoul, Republic of Korea). *PIK3CA* mutations were defined as 11 mutations (C420R, E542K, E545A, E545D [1635G>T only], E545G, E545K, Q546E, Q546R, H1047L, H1047R, and H1047Y), and their efficacy against PI3K inhibitors was verified in the SOLAR-1 trial (NCT02437318) (27). *PIK3CA* mutations were evaluated in the initial tumor tissue and blood samples at the time of diagnosis of metastasis. *PIK3CA* hotspot mutations were detected using amplicon-based targeted NGS in both FFPE tumor samples and paired cfDNA samples.

Targeted NGS is designed to detect variants at a frequency of 0.5%, whereas the ddPCR method is optimized for an average limit of detection (LOD) ranging from 0.05% (1.53 copies) to 0.1% (3 copies). We attempted to detect *ESR1* mutations, even in the early stages, using the ddPCR method, which has a higher sensitivity than targeted NGS. *PIK3CA* mutations are close to each other, as the location of the mutation to be targeted is determined by mutation by 1 base difference. These *PIK3CA* mutations can appear in the form of dual or multiple *PIK3CA* mutations, making it difficult to design primers or probes, so we detected them using the sequencing method.

3.5 Droplet digital PCR

ddPCR was performed on cfDNA obtained from the plasma for *ESR1* mutation detection. To determine the LOD of ddPCR, the following method was established: *ESR1* mutant plasmid DNA samples were serially diluted to concentrations of 0.5%, 0.3%, 0.1%, 0.05%, and 0.01% with *ESR1* wild-type plasmid DNA, and each concentration was subjected to three replicates of ddPCR testing. It was confirmed that up to 0.01% (three copies) of mutant plasmid DNA could be detected. Typically, the input DNA amount was 30 ng; however, in cases where the results were ambiguous, the input DNA amount was increased threefold for re-examination to ensure accurate final results. Due to insufficient sample from one patient, three ddPCR results that required re-examination could not be performed and were excluded from this analysis. Samples that were difficult to interpret clinically and unmatched by the clinical course of the patient were also confirmed through a re-examination process.

3.6 Amplicon-based targeted NGS

To perform amplicon-based targeted NGS using the Illumina platform, we amplified the mutation regions of *PIK3CA* using the *PIK3CA* Mutation PCR Kit (Genopeaks Co., Ltd., Seoul, Republic of Korea). PCR products were purified using AMPure XP beads (Beckman Coulter Inc., Brea, CA, USA) and quantified using a Qubit 4 fluorometer (Thermo Fisher Scientific, Invitrogen, Waltham, MA, USA). Libraries were prepared using the DExV_*PIK3CA* mutation Test Kit (Genopeaks Co., Ltd., Seoul, Republic of Korea) following the manufacturer's protocol. The adapter-ligated libraries were purified and assessed for size using an Agilent 4200 TapeStation (Agilent Technologies, Santa Clara, California, USA), quantified by quantitative PCR, and normalized to a concentration of 4 nM. Pooled libraries were sequenced on an Illumina NextSeq 550Dx sequencer (Illumina, San Diego, CA, USA) using the NextSeq 550Dx High Output Reagent Kit v2.5 (300 cycles) to generate 2–150 bp paired-end reads. Raw data processing involved quality control, alignment to the reference genome, and variant calling using appropriate bioinformatics tools. The identified variants were subsequently annotated and cross-referenced with public databases to determine their clinical significance. The diagnostic cutoff values for each *PIK3CA* mutation type were set differently. This is because differences in reactivity may occur depending on the specific melting temperature value and GC% of the target site, which may cause the experimental reaction sensitivity to vary for each site, resulting in differences in the sequencing coverage and characteristics of each target. The cutoff value for the C420R mutation was set at 1, for H1047L, H1047R, and H1047Y at 0.94, and for E542K, E545K, E545A, E545G, E545D, Q546E, and Q546R at 0.88.

3.7 Statistical analysis

PFS was defined as the interval from the start of palliative first-line ETx to the time of disease progression or death from any cause. Disease-free survival (DFS) was defined as the time until any recurrence after curative surgery. *ESR1* detection to disease progression time was defined as the time between the detection of *ESR1* mutation and the point of clinical progression on radiographic assessment. PFS and DFS analyses were performed using the Kaplan–Meier method and compared using the log-rank test. Means were compared using an independent *t*-test for normally distributed continuous variables. Clearance of *ESR1* mutation was defined as a mutation detected at a specific time point but not detected in subsequent samples. All reported P values were two-sided, and $p < 0.05$ was considered statistically significant. Swimmer plots were created to present the clinical course of the patient and *ESR1* mutation detection. All statistical analyses were performed using the IBM SPSS Statistics for Windows, version 25.0 (IBM Corp., Armonk, NY, USA) and R, version 4.3.2 (The R Project for Statistical Computing, Vienna, Austria).

4. Results

4.1 cfDNA samples

Serial cfDNA samples were collected from the 25 patients according to their hospital visits and blood sampling schedules. A total of 268 samples were analyzed. Most samples were collected at 3-month intervals. The mean interval of blood sampling was 3.3 ± 2.9 months. Three blood samples were collected from two patients at a sampling interval of more than 7 months from the previous sampling. One patient was treated at another hospital during the course of therapy and returned to our hospital 9 months later. In another patient, a blood sample was not collected during a visit where a blood test was not prescribed, and blood was collected during the next visit when a blood test was scheduled.

4.2 Characteristics of the patients

Patient characteristics are summarized in Table 1. The mean age at the initial diagnosis was 45.2 years. Five (20.0%) patients had *de novo* distant metastases. Adjuvant ETx was administered in patients in stage I–III or those in stage IV who had their metastatic lesions disappear after neoadjuvant chemotherapy and subsequently underwent curative surgery. Among these patients, 13 (61.9%) received tamoxifen and 5 (23.8%) received tamoxifen with ovarian suppression. There were 2 (9.5%) who received AI prior to palliative ETx. Chemotherapy was administered to 14 (70.0%) patients. Of the 14 patients who received chemotherapy, 9 (45.0%) received neoadjuvant chemotherapy. Most patients (80.0%) exhibited secondary endocrine resistance. Among the patients with *de novo* metastatic breast cancer, three were endocrine-sensitive. Premenopausal patients at distant metastasis were 16 (64.0%). At the time of distant metastasis, 16 patients (64.0%) were premenopausal. Most premenopausal patients undergo bilateral salpingo-oophorectomy before starting palliative ETx; in this study, only one premenopausal patient underwent bilateral salpingo-oophorectomy 4 months after starting palliative ETx with ovarian suppression. The proportion of patients with bone-only metastasis was 44.0%, and that with visceral metastases was 32%.

Table 1. Patients characteristics (n = 25)

Characteristic	n (%)
Age at diagnosis (years; mean ± SD)	45.2 ± 7.8
Menopausal status at distant metastasis	
Premenopause	16 (64.0)
Postmenopause	9 (36.0)
Distant metastasis	
Recurrent	20 (80.0)
De novo	5 (20.0)
Previous treatment	
Adjuvant endocrine therapy	
Tamoxifen[a]	13 (61.9)
Tamoxifen + ovarian suppression	5 (23.8)
Aromatase inhibitor	2 (9.5)
Tamoxifen → Aromatase inhibitor extension	1 (4.8)
Chemotherapy	
Neoadjuvant	8 (40.0)
AC 4 cycles → Taxane 4 cycles	7
FEC 3 cycles → Taxane 3 cycles[b]	1
Adjuvant	5 (25.0)
AC 4 cycles	3
AC 4 cycles → Taxane 4 cycles	1
CAF 6 cycles	1
Neoadjuvant and adjuvant	1 (5.0)
Neoadjuvant AC 4 cycles → adjuvant Taxane 4 cycles	
No	6 (30.0)
Radiotherapy	
Yes	15 (75.0)

No	5 (25.0)
Endocrine resistance status	
Primary endocrine resistance	2 (10.0)
Secondary endocrine resistance	20 (90.0)
Sensitivity (*de novo* metastasis)	3
Number of metastatic sites	
1	18 (72.0)
2	5 (20.0)
≥ 3	2 (8.0)
Site of distant metastasis	
Non-visceral metastasis	12 (48.0)
Bone only	11
Lymph nodes	1
Visceral metastasis	8 (32.0)
Liver	3
Lung	2
Liver and lung	1
Pleura	2
Non-visceral & visceral metastases	5 (20.0)
Palliative first-line endocrine therapy regimen	
CDK4/6i[c] + Aromatase inhibitor[d]	18 (72.0)
CDK4/6i[c] + Fulvestrant	1 (4.0)
Aromatase inhibitor ± ovarian suppression[e]	4 (16.0)
Fulvestrant	2 (8.0)
Palliative surgery	
No	22 (88.0)
Yes	3 (12.0)
Palliative radiotherapy	
No	16 (64.0)

Yes	9 (36.0)

Data are shown as number (%), not otherwise specified

Abbreviations: SD, standard deviation; AC, anthracycline and cyclophosphamide; FEC, fluorouracil, epirubicin, and cyclophosphamide; CAF, cyclophosphamide, adriamycin and fluorouracil; CDK4/6i, inhibitor of cyclin-dependent kinases 4 and 6

[a] One patient with *de novo* metastasis in the lymph node underwent surgery with curative intent after neoadjuvant chemotherapy, and tamoxifen was used as adjuvant ETx.

[b] Neoshorter study (NCT02001506)

[c] Palbociclib was used as a CDK4/6 inhibitor in all cases.

[d] In combination with CDK4/6i, letrozole was used as an aromatase inhibitor in all cases.

[e] One premenopausal patient initially began treatment with an aromatase inhibitor and gonadotropin-releasing hormone agonist. After 4 months of treatment, the patient underwent bilateral salpingo-oophorectomy and then used only aromatase inhibitor.

4.3 Treatment

Most patients (72.0%) received CDK4/6i + AI as palliative first-line ETx, followed by AI (16.0%), fulvestrant (8.0%), and CDK4/6i + fulvestrant (4.0%) (Table 1). Palliative surgery and radiotherapy were performed in three (12.0%) and nine (36.0 %) patients, respectively. Two patients underwent both palliative radiotherapy and palliative surgery. The median PFS was 43.4 months (range, 3.6–69.3 months).

The ETx regimen for each patient is shown in Figure 2. Six patients were treated with a single endocrine agent as first-line palliative ETx, which is not the current standard regimen. Patients AMCM014 was treated with letrozole alone as the first-line ETx. The patient developed distant metastasis as a contralateral axillary lymph node. The treatment was discussed at a multidisciplinary clinic. Surgical resection was possible; however, the patient was expected to respond well to the ETx. Therefore, treatment with ETx was first attempted, and if the response was favorable, the possibility of radiation therapy to the residual disease was discussed. The patient received letrozole alone and palliative radiotherapy. After 9 months of letrozole therapy, the disease progressed. The patient was administered abemaciclib and fulvestrant. Patient AMCM018 developed painful bone metastasis as a large mass with destruction of the sternum. This case was discussed at a multidisciplinary clinic. The patient was advised to start letrozole, a gonadotropin-releasing hormone agonist, and to receive palliative radiotherapy. Patient AMCM027 received only anastrozole as first-line ETx. The medical records at the time of distant metastasis did not specify why a single agent was used. However, this patient refused CDK4/6i even after disease progression; therefore, fulvestrant alone was used as a third-line ETx. Patient DNAM011 had bone metastases with a low tumor burden, and the use of fulvestrant alone as first-line ETx was discussed in a multidisciplinary clinic. Patient DNAM039 had a single bone lesion and underwent salvage stereotactic body radiation therapy to that area. Subsequently, the use of fulvestrant only or fulvestrant + CDK4/6i was discussed with the physician and the patient, and the patient decided to receive fulvestrant only. Patient AMCM007 initially presented with bilateral breast cancer with skin involvement and bone metastasis. The surgeon decided to administer palliative anastrozole. After 3 months of

treatment, the bone lesion was in a stable disease state on radiological examination, and the skin lesion improved on physical examination. Therefore, the patient decided to continue treatment, with follow-up imaging to determine whether surgery was needed.

Five patients were enrolled in clinical trials for the second and subsequent lines of ETx. Patient DNAM014 was treated with atezolizumab + ipatasertib + fulvestrant as second-line ETx. The last four patients were enrolled in clinical trials involving oral SERD. Patients DNAM024 and DNAM051 were treated with giredestrant + ipatasertib and imlunestrant as second-line ETx, respectively. Patient DNAM033 was treated with borestrant as a third-line ETx, and patient DNAM043 started using imlunestrant as a second-line ETx on the last follow-up date. None of the patients in this study were administered PI3K inhibitors.

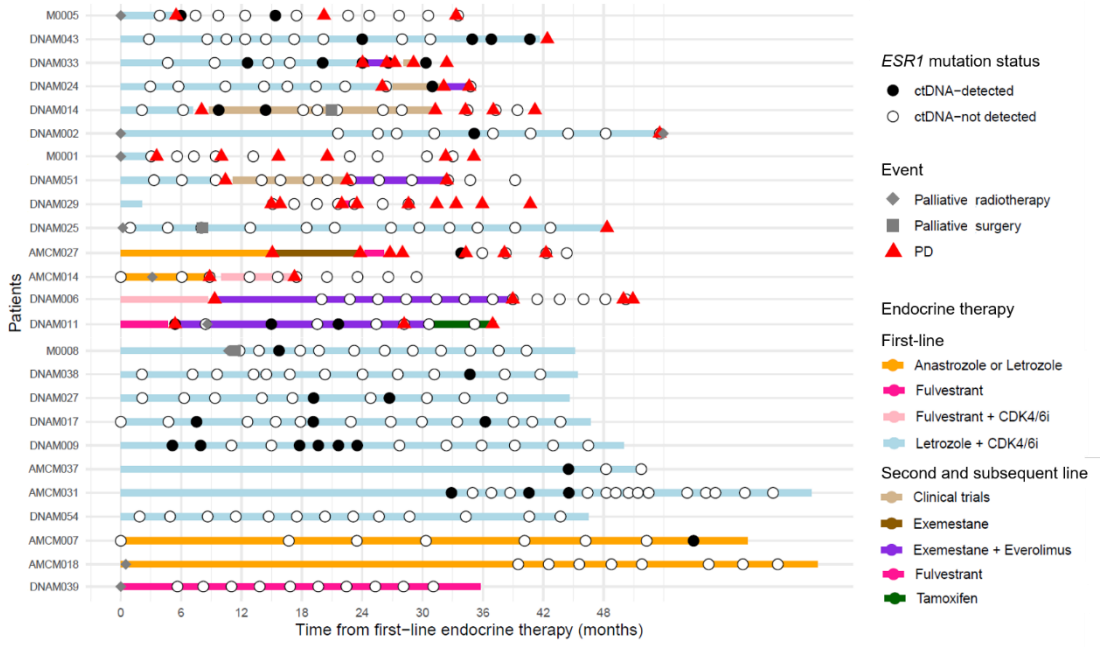

Figure 2. Swimmer plot presenting *ESR1* mutation status and clinical information of individual patients after palliative first-line endocrine therapy.

PD, disease progression; CDK4/6i, inhibitor of cyclin-dependent kinases 4 and 6.

Patients who received palliative radiotherapy before palliative first-line endocrine therapy were indicated at the start of palliative endocrine therapy.

4.4 *ESR1* mutation

Longitudinal analyses of ctDNAs in the plasma of each patient were performed. The median follow-up period from first-line ETx was 44.6 months (range, 32.5–69.3 months). Among the 25 patients, b*ESR1* mutations were detected in 16 (64.0%) at any time point during first-line ETx. Among them, there were 3 (18.8%) patients whose *ESR1* mutations were continuously detected until the last cfDNA examination. Overall, there were 53 samples in which *ESR1* mutations were detected. The most common mutation was D538G (17/53), followed by S643P (14/53), Y537C (12/53), Y537N (6/53), Y537S (2/53), and E380Q (2/53). Multiple mutations were detected in 11 (68.8%) patients. The ddPCR results and plots for patients with *ESR1* mutations are presented in Figures 3–35.

***ESR1* D538G – DNAM043**

Well	Sample	cp	cp/20ul	droplet
A01	DW	-	0	20308
C01	synPWT	1000cp	0	21017
D01	D538G	1000cp	706	21576
D04	3m	30ng	0	22062
E04	9m	30ng	0	13089
F04	11m	30ng	0	19544
G04	12m	30ng	0	21014
H04	14m	30ng	0	21392

Well	Sample	cp	cp/20ul	droplet
A01	DW	-	0	15461
B01	gDNA	10ng	0	14660
C01	synPWT	1000cp	0	15566
D01	D538G	1000cp	754	16596
E01	17m	30ng	0	17607
F01	20m	30ng	0	15647
G01	24m	30ng	0	16166
H01	28m	30ng	0	15307
A02	31m	30ng	0	18824
B02	34m	30ng	7.4	18936
C02	36m	30ng	0	19075
D02	40m	30ng	5.2	18220

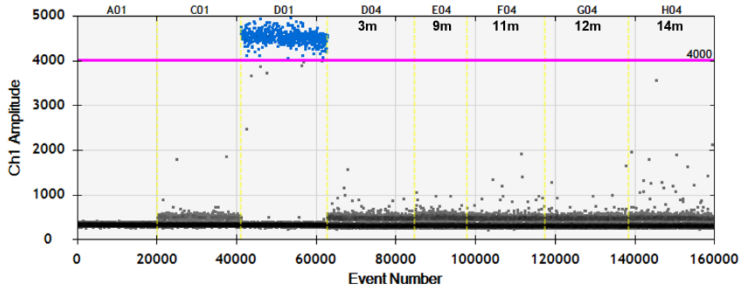

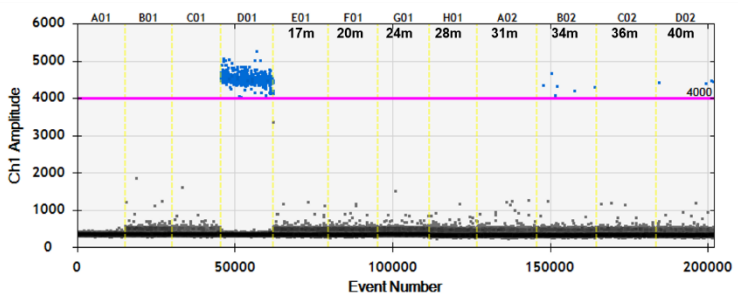

Figure 3. *ESR1* D538G mutation droplet digital polymerase chain reaction result and plot for the DNAM043 patients.

DW, distilled water; synPWT, synthetic wild-type plasmid.

***ESR1* D538G – DNAM009**

Well	Sample	cp	cp/20ul	droplet
A01	DW	-	0	19853
B01	gDNA	10ng	0	20925
D01	D538G	1000cp	770	21269
G01	4m	30ng	2.4	20039
H01	7m	30ng	2.2	21491
A02	10m	30ng	0	20205
B02	14m	30ng	0	21040
C02	17m	30ng	0	18999
D02	19m	30ng	3.6	19309
E02	21m	30ng	0	18446
F02	23m	30ng	1.2	18744
G02	27m	30ng	2.2	21585
H02	31m	30ng	0	21567
A03	35m	30ng	0	20689
B03	37m	30ng	0	20213
C03	41m	30ng	0	21440
D03	44m	30ng	0	21029

4m, 7m, 23m, 27m sample re-examination

Well	Sample	cp	cp/20ul	droplet
A08	DW	-	0	20961
B08	gDNA	10ng	0	20516
C08	D538G	1000cp	860	19971
F09	4m	90ng	6.6	21411
G09	7m	90ng	5.8	20563
H09	23m	90ng	3.4	20556
A10	27m	90ng	0	18879

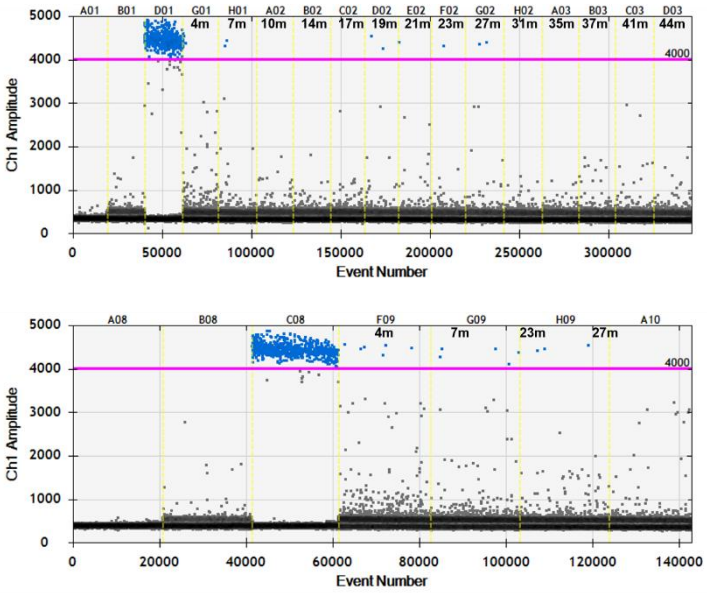

Figure 4. *ESR1* D538G mutation droplet digital polymerase chain reaction results and plot for the DNAM009 patients.

DW, distilled water.

***ESR1* D538G – DNAM011**

Well	Sample	cp	cp/20ul	droplet
A01	DW	-	0	19853
B01	gDNA	10ng	0	20925
C01	synPWT	1000cp	0	21709
D01	D538G	1000cp	770	21269
E03	3m	30ng	2.4	19495
F03	6m	30ng	0	20822
G03	12m	30ng	0	19600
H03	17m	30ng	0	20932
A04	19m	30ng	0	12398
B04	23m	30ng	0	20930
C04	26m	30ng	0	20910
D04	28m	30ng	0	18792
E04	33m	30ng	0	19551

3m sample re-examination

Well	Sample	cp	cp/20ul	droplet
A08	DW	-	0	20961
B08	gDNA	10ng	0	20516
C08	D538G	1000cp	860	19971
B10	3m	90ng	3.6	19171

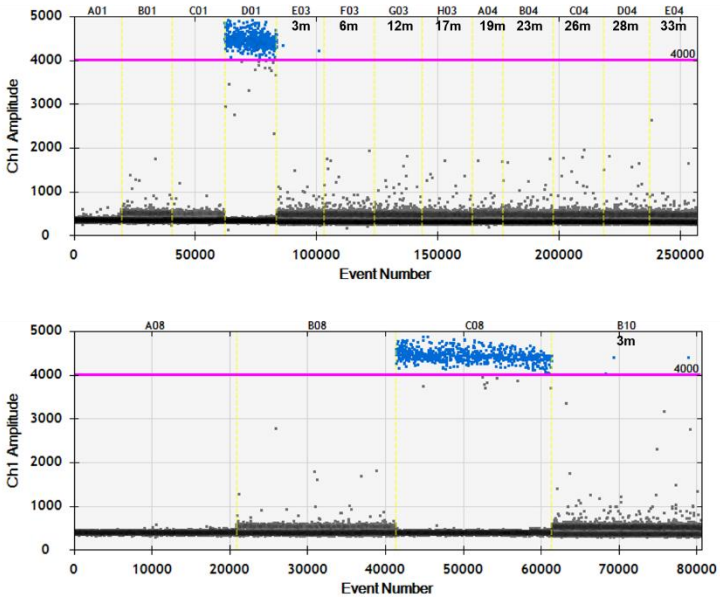

Figure 5. *ESR1* D538G mutation droplet digital polymerase chain reaction results and plot for the DNAM011 patient.

DW: distilled water; synPWT: synthetic wild-type plasmid.

***ESR1* D538G – DNAM014**

Well	Sample	cp	cp/20ul	droplet
A01	DW	-	0	19853
B01	gDNA	10ng	0	20925
D01	D538G	1000cp	770	21269
F04	**2m**	30ng	0	20634
G04	**6m**	30ng	0	20723
H04	**9m**	30ng	**4.6**	20735

Well	Sample	cp	cp/20ul	droplet
A09	DW	-	0	21338
B09	gDNA	10ng	0	22003
D09	D538G	1000cp	840	21154
E09	**14m**	30ng	**1.2**	21327
F09	**18m**	30ng	0	21333
G09	**19m**	30ng	0	21763
H09	**21m**	30ng	0	21243
A10	**26m**	30ng	0	20490
B10	**27m**	30ng	0	20535
C10	**34m**	30ng	0	20517
D10	**37m**	30ng	0	21740
E10	**38m**	30ng	0	21336

14m sample re-examination

Well	Sample	cp	cp/20ul	droplet
A08	DW	-	0	20961
B08	gDNA	10ng	0	20516
C08	D538G	1000cp	860	19971
C10	**14m**	**90ng**	**4.8**	19285

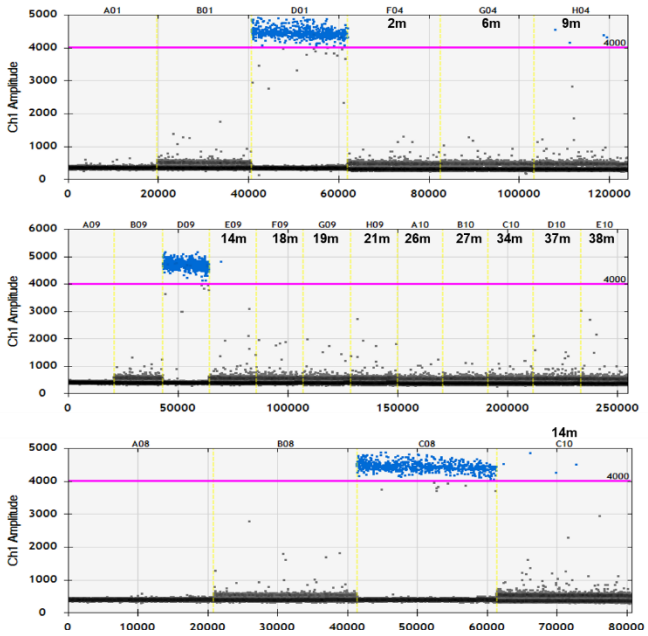

Figure 6. *ESR1* D538G mutation droplet digital polymerase chain reaction results and plot for the DNAM014 patient.

DW, distilled water.

***ESR1* D538G – DNAM017**

Well	Sample	cp	cp/20ul	droplet
A09	DW	-	0	21338
B09	gDNA	10ng	0	22003
D09	D538G	1000cp	840	21154
F10	2m	30ng	0	21703
G10	7m	30ng	0	21764
H10	10m	30ng	1.2	20911
A11	15m	30ng	0	21236
B11	18m	30ng	0	21596
C11	20m	30ng	0	20772
D11	22m	30ng	6.8	20970
E11	25m	30ng	0	21082
F11	29m	30ng	0	21275
G11	32m	30ng	0	20535
H11	36m	30ng	0	21318
A12	38m	30ng	1	21881
B12	40m	30ng	0	20991
C12	42m	30ng	0	21639
D12	45m	30ng	0	22143

10m, 38m sample re-examination

Well	Sample	cp	cp/20ul	droplet
A08	DW	-	0	20961
B08	gDNA	10ng	0	20516
C08	D538G	1000cp	860	19971
D10	10m	90ng	4.6	20158
E10	38m	90ng	3.6	19207

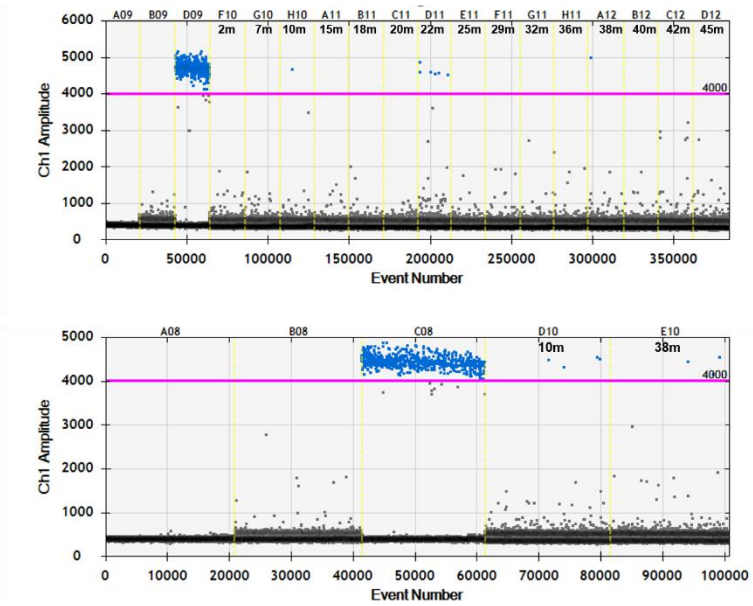

Figure 7. *ESR1* D538G mutation droplet digital polymerase chain reaction results and plot for the DNAM017 patient.

DW, distilled water.

***ESR1* D538G – DNAM024**

Well	Sample	cp	cp/20ul	droplet
A09	DW	-	0	21338
B09	gDNA	10ng	0	22003
D09	D538G	1000cp	840	21154
E12	**4m**	30ng	0	20617
F12	**6m**	30ng	1	21770
G12	**11m**	30ng	0	21775
H12	**15m**	30ng	0	21529

Well	Sample	cp	cp/20ul	droplet
A01	DW	-	0	22234
B01	gDNA	10ng	0	20823
D01	D538G	1000cp	842	20848
E01	**17m**	30ng	0	21132
F01	**20m**	30ng	0	21090
G01	**23m**	30ng	0	21194
H01	**27m**	30ng	1	22121
A02	**32m**	30ng	2.4	20073
B02	**36m**	30ng	0	21545

6m, 27m, 32m sample re-examination

Well	Sample	cp	cp/20ul	droplet
A08	DW	-	0	20961
B08	gDNA	10ng	0	20516
C08	D538G	1000cp	860	19971
F10	**6m***	90ng	1.2	19281
G10	**27m**	90ng	0	21059
H10	**32m**	90ng	5.6	20834

*Only 1 droplet emerged from 90ng input and judged to be negative

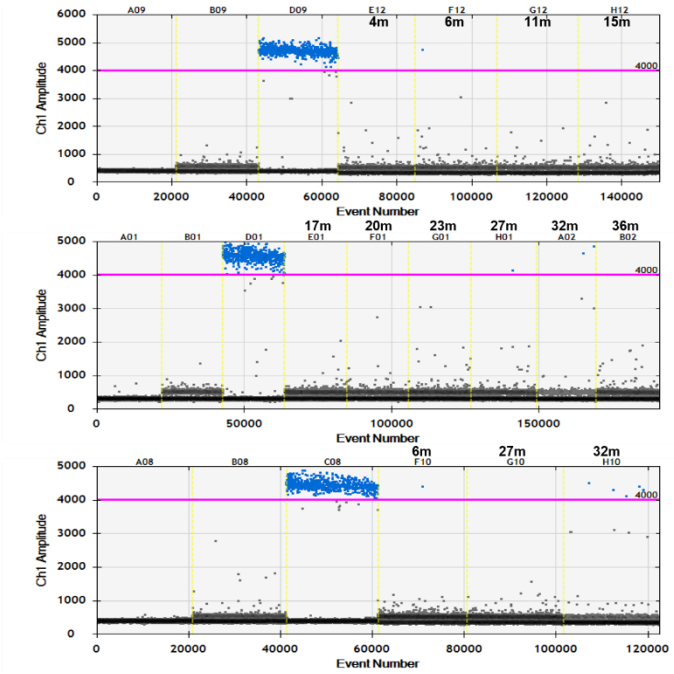

Figure 8. *ESR1* D538G mutation droplet digital polymerase chain reaction results and plot for the DNAM024 patient.

DW, distilled water.

***ESR1* D538G – M0005**

Well	Sample	cp	cp/20ul	droplet
A01	DW	-	0	20924
B01	gDNA	10ng	0	21347
D01	D538G	1000cp	848	21590
C05	**4m**	30ng	0	22008
D05	**6m**	30ng	0	22291
E05	**7m**	30ng	0	21130
F05	**10m**	30ng	0	20497
G05	**12m**	30ng	0	21340
H05	**15m**	30ng	**1.2**	21312
A06	**17m**	30ng	0	14785
B06	**23m**	30ng	0	20139
C06	**36m**	30ng	0	21903
D06	**39m**	30ng	0	20620
E06	**42m**	30ng	0	21676
F06	**45m**	30ng	**1**	22131

15m, 45m sample re-examination

Well	Sample	cp	cp/20ul	droplet
A08	DW	-	0	20961
B08	gDNA	10ng	0	20516
C08	D538G	1000cp	860	19971
H11	**15m**	90ng	**2.4**	19566
A12	**45m**	90ng	0	19206

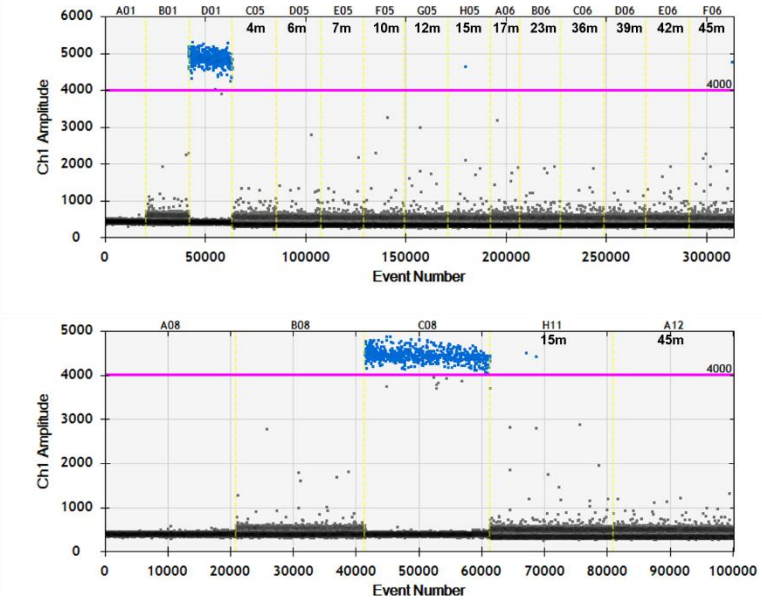

Figure 9. *ESR1* D538G mutation droplet digital polymerase chain reaction results and plot for the M0005 patient.

DW, distilled water.

***ESR1* D538G – M0008**

Well	Sample	cp	cp/20ul	droplet
A01	DW	-	0	20924
B01	gDNA	10ng	0	21347
D01	D538G	1000cp	848	21590
G06	**2m**	30ng	0	21355
H06	**4m**	30ng	0	21196

Well	Sample	cp	cp/20ul	droplet
A01	DW	-	0	20466
B01	gDNA	10ng	0	22182
C01	D538G	1000cp	852	21882
D01	**6m**	30ng	**1.2**	21328
E01	**8m**	30ng	0	21742
F01	**10m**	30ng	**1**	22183
G01	**14m**	30ng	0	21538
H01	**17m**	30ng	0	20714
A02	**19m**	30ng	0	22528
B02	**22m**	30ng	0	22298
C02	**38m**	30ng	0	21001
D02	**41m**	30ng	0	20982
E02	**44m**	30ng	0	22692

6m, 10m sample re-examination

Well	Sample	cp	cp/20ul	droplet
A08	DW	-	0	20961
B08	gDNA	10ng	0	20516
C08	D538G	1000cp	860	19971
B12	**6m**	90ng	**2.6**	18353
C12	**10m***	90ng	1.2	19742

*Only 1 droplet emerged from 90ng input and judged to be negative

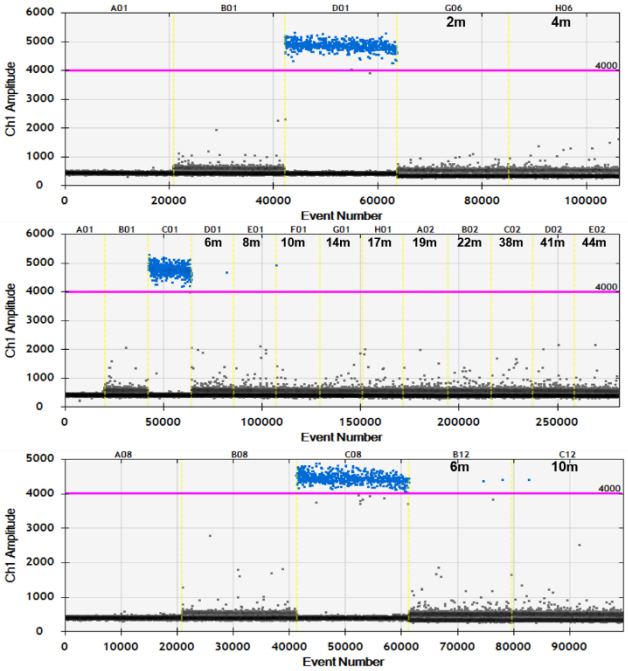

Figure 10. *ESR1* D538G mutation droplet digital polymerase chain reaction results and plot for the M0008 patient.

DW, distilled water.

***ESR1* D538G – AMCM007**

Well	Sample	cp	cp/20ul	droplet
A01	DW	-	0	20466
B01	gDNA	10ng	0	22182
C01	D538G	1000cp	852	21882
F02	**3m**	30ng	0	22386
G02	**20m**	30ng	0	21272
H02	**26m**	30ng	0	22798
A03	**33m**	30ng	1.2	21365
B03	**43m**	30ng	0	20878
C03	**49m**	30ng	0	20923
D03	**55m**	30ng	0	20366
E03	**60m**	30ng	3.4	20972

33m, 60m sample re-examination

Well	Sample	cp	cp/20ul	droplet
A08	DW	-	0	20961
B08	gDNA	10ng	0	20516
C08	D538G	1000cp	860	19971
D12	**33m***	90ng	1.2	19690
E12	**60m**	90ng	8	20550

*Only 1 droplet emerged from 90ng input and judged to be negative

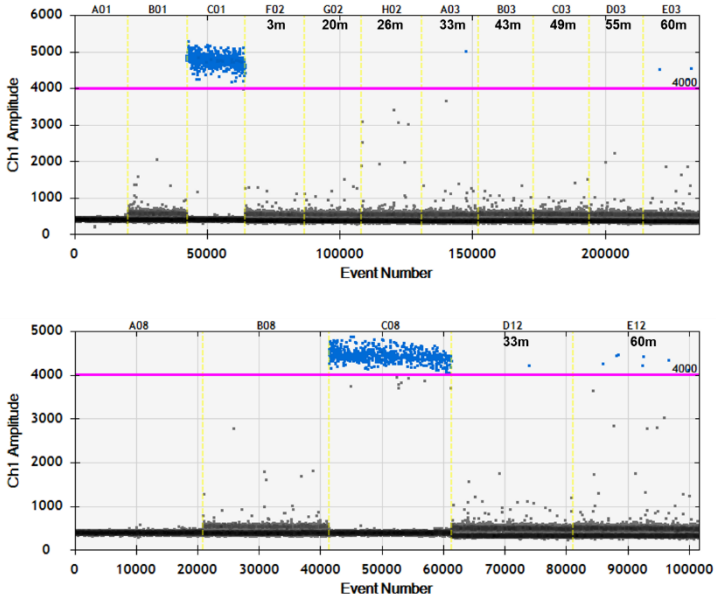

Figure 11. *ESR1* D538G mutation droplet digital polymerase chain reaction results and plot for the AMCM007 patient.

DW, distilled water.

***ESR1* S463P – AMCM031**

Well	Sample	cp	cp/20ul	droplet
A03	DW	-	0	20167
B03	gDNA	10ng	0	18465
D03	S463P	1000cp	1026	19205
H03	**32m**	30ng	0	19860
A04	**34m**	30ng	0	20085
B04	**36m**	30ng	1.2	19957
C04	**38m**	30ng	0	19404
D04	**39m**	30ng	1.2	20099
E04	**43m**	30ng	0	20102
F04	**45m**	30ng	0	19613
G04	**47m**	30ng	0	20358
H04	**48m**	30ng	0	18915
A05	**49m**	30ng	0	20072
B05	**50m**	30ng	0	20398
C05	**51m**	30ng	0	17997
D05	**55m**	30ng	0	12853
E05	**56m**	30ng	1.2	19370
F05	**57m**	30ng	0	18908
G05	**60m**	30ng	0	19542
H05	**62m**	30ng	0	19924

36m, 47m, 56m sample re-examination

Well	Sample	cp	cp/20ul	droplet
A07	DW	-	0	21555
B07	gDNA	10ng	0	20540
D07	S463P	1000cp	1158	21898
E07	**36m**	90ng	0	21431
F07	**39m**	90ng	4.6	20594
G07	**56m**	90ng	0	20253

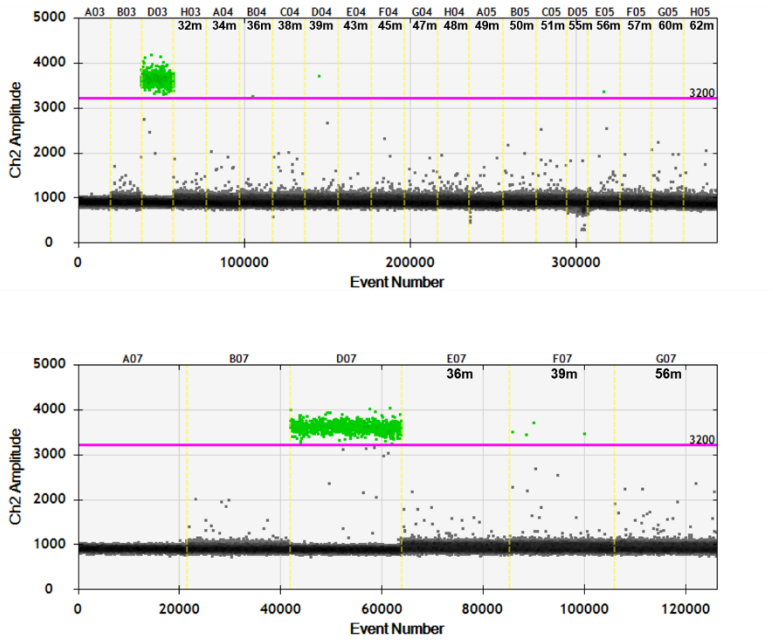

Figure 12. *ESR1* S643P mutation droplet digital polymerase chain reaction results and plot for the AMCM031 patient.

DW, distilled water.

***ESR1* S463P – DNAM043**

Well	Sample	cp	cp/20ul	droplet
A03	DW	-	0	20167
B03	gDNA	10ng	0	18465
C03	Y537N	1000cp	0	19609
D03	S463P	1000cp	1026	19205
D06	**3m**	30ng	0	20428
E06	**9m**	30ng	0	19749
F06	**11m**	30ng	0	20151
G06	**12m**	30ng	0	20425
H06	**14m**	30ng	0	20251

Well	Sample	cp	cp/20ul	droplet
A01	DW	-	0	20601
B01	gDNA	10ng	0	20605
C01	Y537N	1000cp	0	20011
D01	S463P	1000cp	1082	19800
E01	**17m**	30ng	0	19652
F01	**20m**	30ng	0	18845
G01	**24m**	30ng	3.6	19846
H01	**28m**	30ng	0	18748
A02	**31m**	30ng	0	21183
B02	**34m**	30ng	0	19529
C02	**36m**	30ng	0	19813
D02	**40m**	30ng	0	19029

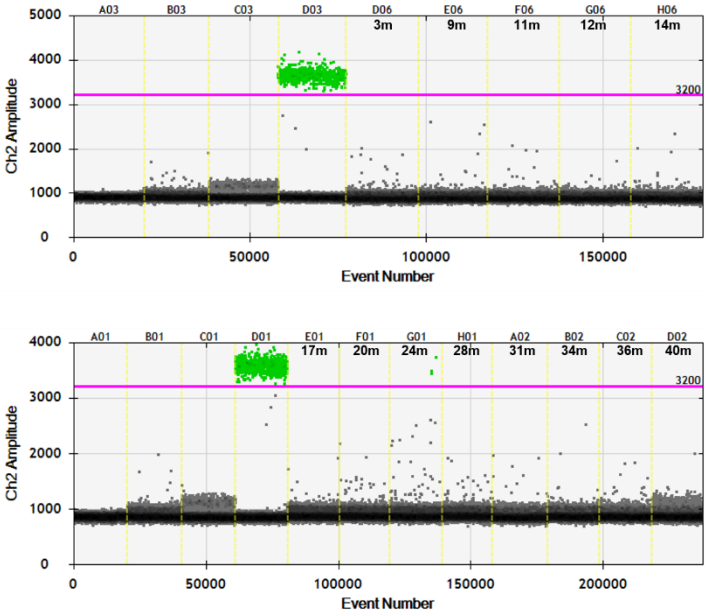

Figure 13. *ESR1* S643P mutation droplet digital polymerase chain reaction results and plot for the DNAM043 patient.

DW, distilled water.

***ESR1* S463P – DNAM009**

Well	Sample	cp	cp/20ul	droplet
A01	DW	-	0	20860
B01	gDNA	10ng	0	21035
D01	S463P	1000cp	1158	20856
G01	4m	30ng	9.6	21869
H01	7m	30ng	0	20787
A02	10m	30ng	0	20060
B02	14m	30ng	0	18997
C02	17m	30ng	1.2	20621
D02	19m	30ng	1.2	19818
E02	21m	30ng	1.2	21053
F02	23m	30ng	0	21755
G02	27m	30ng	0	20761
H02	31m	30ng	0	20588
A03	35m	30ng	0	18911
B03	37m	30ng	0	19443
C03	41m	30ng	0	21580
D03	44m	30ng	1.2	20793

17m, 19m, 21m sample re-examination

Well	Sample	cp	cp/20ul	droplet
A07	DW	-	0	21555
B07	gDNA	10ng	0	20540
D07	S463P	1000cp	1158	21898
G08	17m	90ng	2.2	21448
H08	19m	90ng	3.2	22345
A09	21m	90ng	3.4	20551

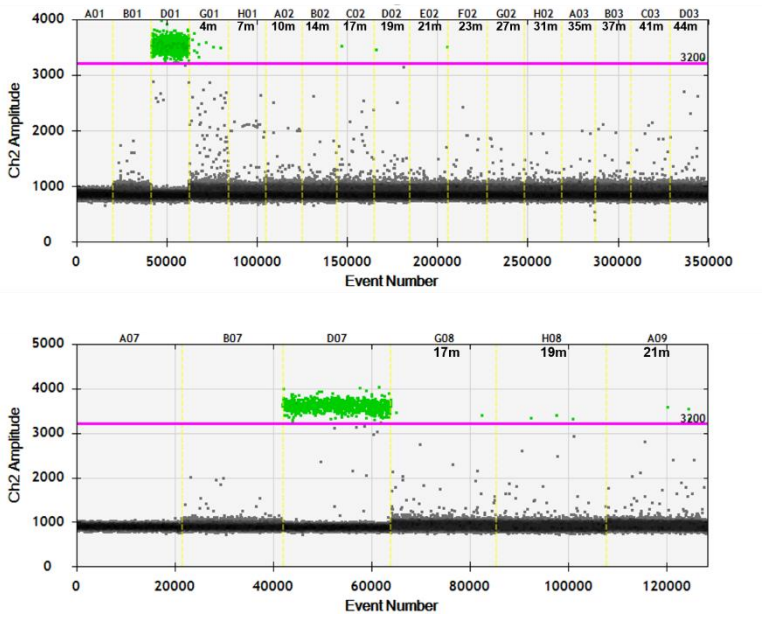

Figure 14. *ESR1* S643P mutation droplet digital polymerase chain reaction results and plot for the DNAM009 patients.

DW, distilled water.

***ESR1* S463P – DNAM011**

Well	Sample	cp	cp/20ul	droplet
A01	DW	-	0	20860
B01	gDNA	10ng	0	21035
C01	Y537N	1000cp	0	19749
D01	S463P	1000cp	1158	20856
E03	**3m**	30ng	0	20479
F03	**6m**	30ng	0	13541
G03	**12m**	30ng	2.2	21586
H03	**17m**	30ng	0	20902
A04	**19m**	30ng	1.2	20066
B04	**23m**	30ng	0	20714
C04	**26m**	30ng	1.2	20959
D04	**28m**	30ng	0	21889
E04	**33m**	30ng	0	19705

12m, 19m, 26m sample re-examination

Well	Sample	cp	cp/20ul	droplet
A07	DW	-	0	21555
B07	gDNA	10ng	0	20540
C07	Y537N	1000cp	0	21261
D07	S463P	1000cp	1158	21898
D09	**12m**	90ng	3.4	20250
E09	**19m**	90ng	2.2	20836
F09	**26m**	90ng	0	21271

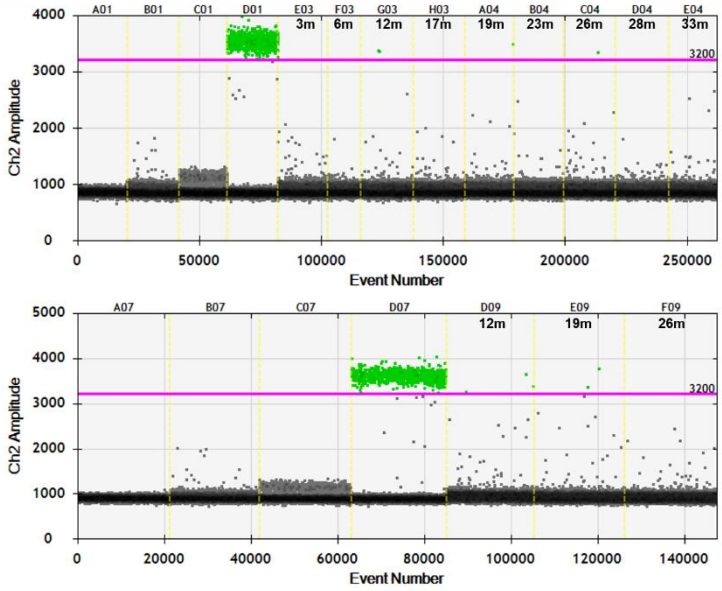

Figure 15. *ESR1* S643P mutation droplet digital polymerase chain reaction results and plot for the DNAM011 patient.

DW, distilled water.

***ESR1* S463P – DNAM014**

Well	Sample	cp	cp/20ul	droplet
A01	DW	-	0	20860
B01	gDNA	10ng	0	21035
D01	S463P	1000cp	1158	20856
F04	**2m**	30ng	0	20851
G04	**6m**	30ng	0	19048
H04	**9m**	30ng	7	20148

Well	Sample	cp	cp/20ul	droplet
A07	DW	-	0	21866
B07	gDNA	10ng	0	22567
D07	S463P	1000cp	1150	21917
E07	**14m**	30ng	2.2	22011
F07	**18m**	30ng	0	21988
G07	**19m**	30ng	0	21759
H07	**21m**	30ng	0	22324
A08	**26m**	30ng	0	21408
B08	**27m**	30ng	0	22081
C08	**34m**	30ng	1	21445
D08	**37m**	30ng	0	21742
E08	**38m**	30ng	0	20677

34m sample re-examination

Well	Sample	cp	cp/20ul	Droplet
A07	DW	-	0	21555
B07	gDNA	10ng	0	20540
D07	S463P	1000cp	1158	21898
A10	**34m**	90ng	0	0

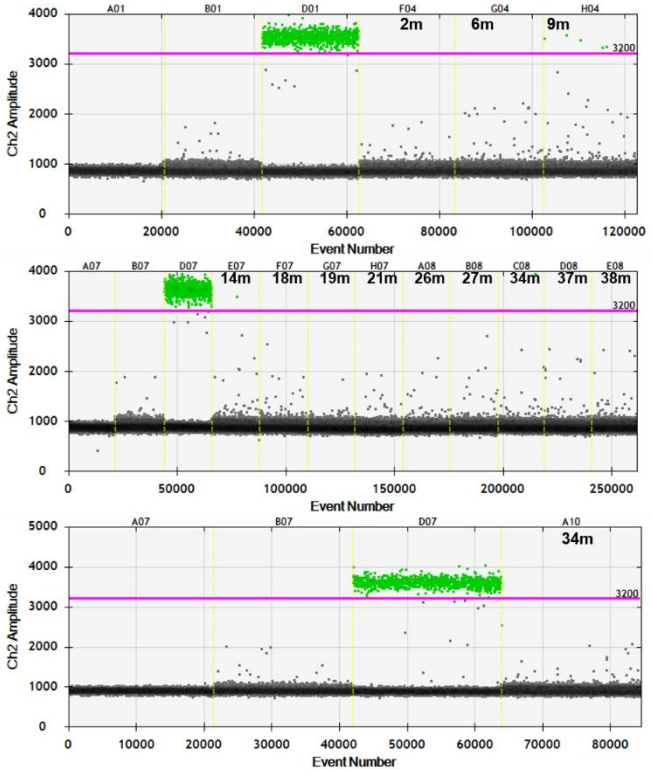

Figure 16. *ESR1* S643P mutation droplet digital polymerase chain reaction results and plot for DNAM014 patient.

DW, distilled water.

***ESR1* S463P – DNAM017**

Well	Sample	cp	cp/20ul	droplet
A07	DW	-	0	21866
B07	gDNA	10ng	0	22567
D07	S463P	1000cp	1150	21917
F08	2m	30ng	0	21805
G08	7m	30ng	0	20715
H08	10m	30ng	4.4	21105
A09	15m	30ng	0	22542
B09	18m	30ng	1.2	21374
C09	20m	30ng	0	21991
D09	22m	30ng	3	22839
E09	25m	30ng	0	22564
F09	29m	30ng	0	20921
G09	32m	30ng	0	22659
H09	36m	30ng	0	21078
A10	38m	30ng	0	21405
B10	40m	30ng	0	20845
C10	42m	30ng	0	21829
D10	45m	30ng	0	20634

18m sample re-examination

Well	Sample	cp	cp/20ul	droplet
A07	DW	-	0	21555
B07	gDNA	10ng	0	20540
D07	S463P	1000cp	1158	21898
C10	18m	90ng	0	0

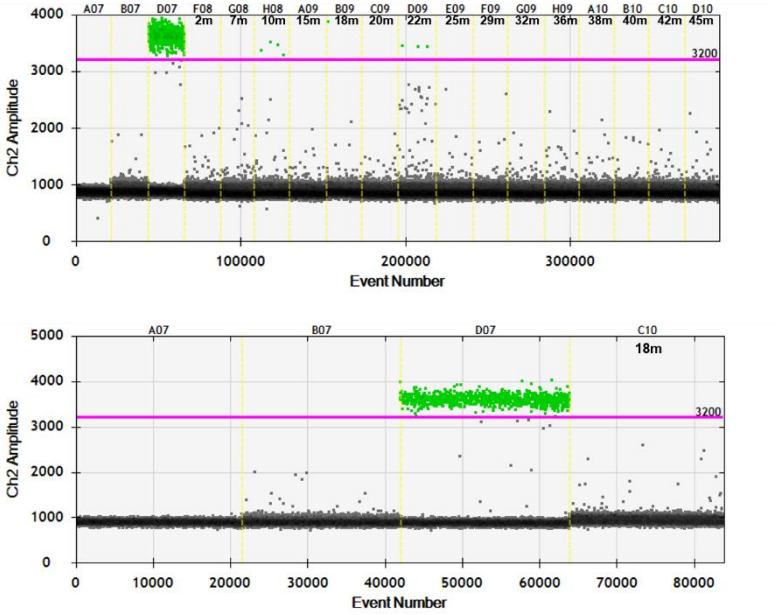

Figure 17. *ESR1* S643P mutation droplet digital polymerase chain reaction results and plot for the DNAM017 patient.

DW, distilled water.

***ESR1* S463P – DNAM024**

Well	Sample	cp	cp/20ul	droplet
A07	DW	-	0	21866
B07	gDNA	10ng	0	22567
D07	S463P	1000cp	1150	21917
E10	4m	30ng	1.2	19977
F10	6m	30ng	0	20158
G10	11m	30ng	0	21971
H10	15m	30ng	0	20695
A11	17m	30ng	1	22210
B11	20m	30ng	0	22273
C11	23m	30ng	0	20846
D11	27m	30ng	0	12161
E11	32m	30ng	1.2	21099
F11	36m	30ng	0	21935

4m, 17m, 27m sample re-examination

Well	Sample	cp	cp/20ul	droplet
A07	DW	-	0	21555
B07	gDNA	10ng	0	20540
D07	S463P	1000cp	1158	21898
E10	4m	90ng	0	0
F10	17m	90ng	0	0
G10	27m	90ng	0	0

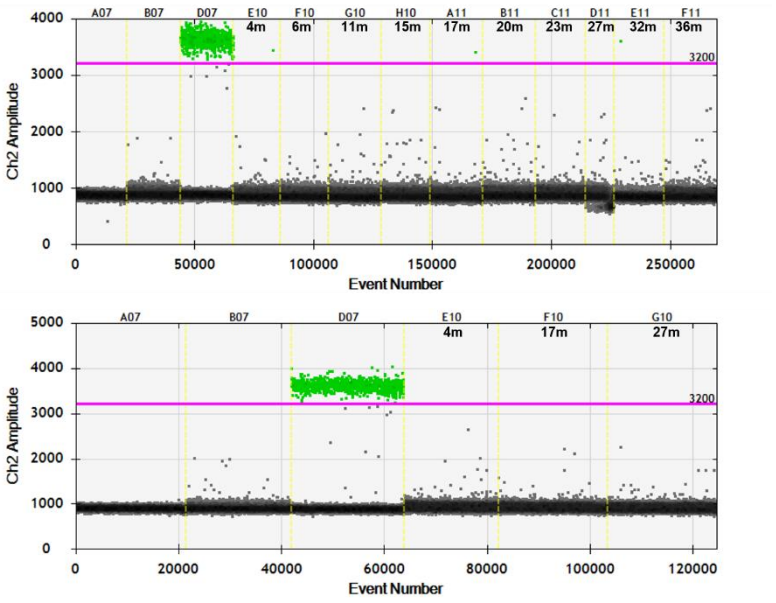

Figure 18. *ESR1* S643P mutation droplet digital polymerase chain reaction results and plot for the DNAM024 patient.

DW, distilled water.

***ESR1* S463P – DNAM027**

Well	Sample	Cp	cp/20ul	droplet
A01	DW	-	0	19721
B01	gDNA	10ng	0	17894
D01	S463P	1000cp	1114	20492
G01	**4m**	30ng	0	18348
H01	**8m**	30ng	0	19534
A02	**11m**	30ng	0	20044
B02	**16m**	30ng	0	18651
C02	**19m**	30ng	0	18999
D02	**21m**	30ng	5.2	18401
E02	**27m**	30ng	0	20600
F02	**29m**	30ng	0	20632
G02	**32m**	30ng	1.2	19846
H02	**35m**	30ng	1.2	21079

Well	Sample	cp	cp/20ul	droplet
A09	DW	-	0	21112
B09	gDNA	10ng	0	20626
D09	S463P	1000cp	1122	20418
E09	**39m**	30ng	0	22649

32m sample re-examination

Well	Sample	cp	cp/20ul	droplet
A09	DW	-	0	21344
B09	gDNA	10ng	0	22386
D09	S463P	1000cp	1228	22182
D10	**32m**	90ng	0	21651

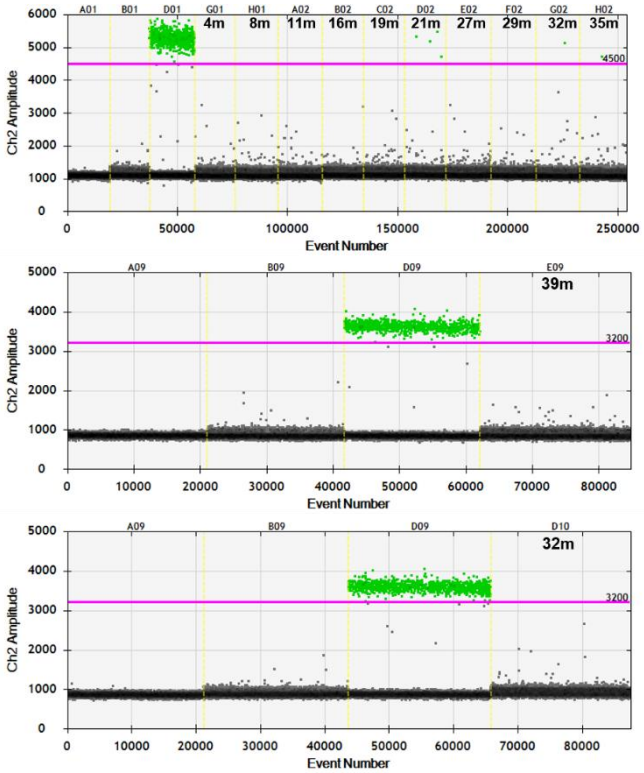

Figure 19. *ESR1* S643P mutation droplet digital polymerase chain reaction results and plot for the DNAM027 patient.

DW, distilled water.

***ESR1* Y537N – AMCM037**

Well	Sample	cp	cp/20ul	droplet
A03	DW	-	0	20167
B03	gDNA	10ng	0	18465
C03	Y537N	1000cp	1254	19609
A06	44m	30ng	1.2	20008
B06	47m	30ng	0	19129
C06	51m	30ng	0	20834

44m sample re-examination

Well	Sample	cp	cp/20ul	droplet
A07	DW	-	0	21555
B07	gDNA	10ng	0	20540
C07	Y537N	1000cp	1278	21261
H07	44m	90ng	4.2	22110

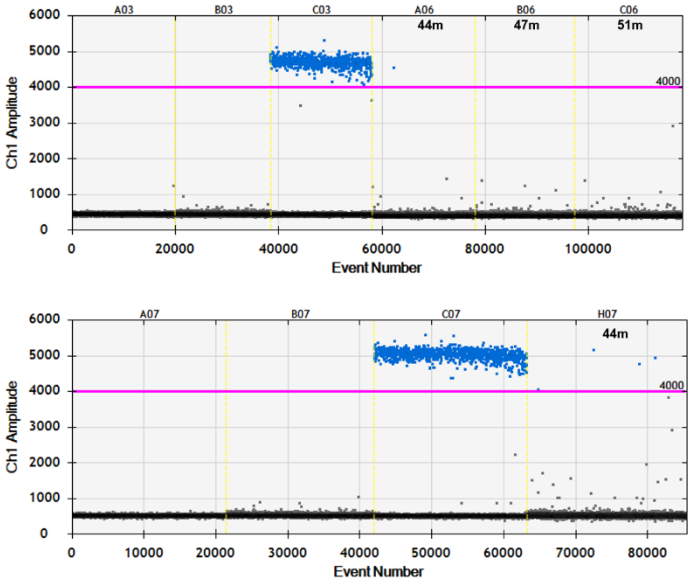

Figure 20. *ESR1* Y537N mutation droplet digital polymerase chain reaction results and plot for the AMCM037 patients.

DW, distilled water.

***ESR1* Y537N – DNAM043**

Well	Sample	cp	cp/20ul	droplet
A03	DW	-	0	20167
B03	gDNA	10ng	0	18465
C03	Y537N	1000cp	1254	19609
D06	3m	30ng	0	20428
E06	9m	30ng	0	19749
F06	11m	30ng	0	20151
G06	12m	30ng	0	20425
H06	14m	30ng	0	20251

Well	Sample	cp	cp/20ul	droplet
A01	DW	-	0	20601
B01	gDNA	10ng	0	20605
C01	Y537N	1000cp	1322	20011
E01	17m	30ng	0	19652
F01	20m	30ng	0	18845
G01	24m	30ng	0	19846
H01	28m	30ng	0	18748
A02	31m	30ng	0	21183
B02	34m	30ng	0	19529
C02	36m	30ng	22	19813
D02	40m	30ng	384	19029

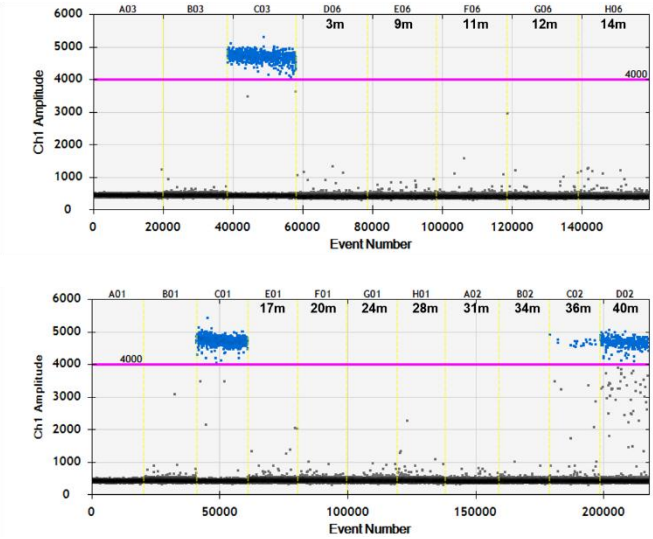

Figure 21. *ESR1* Y537N mutation droplet digital polymerase chain reaction results and plot for the DNAM043 patients.

DW, distilled water.

***ESR1* Y537N – DNAM002**

Well	Sample	cp	cp/20ul	droplet
A09	DW	-	0	18973
B09	gDNA	10ng	0	19054
C09	Y537N	1000cp	1166	20200
D10	**22m**	30ng	0	20469
E10	**26m**	30ng	0	19947
F10	**27m**	30ng	0	21024
G10	**31m**	30ng	0	21161
H10	**35m**	30ng	2.2	20801
A11	**37m**	30ng	0	21160
B11	**41m**	**30ng**	1.2	21098
C11	**43m**	30ng	0	19981
D11	**47m**	30ng	0	21117
E11	**52m**	30ng	0	19965

41m sample re-examination

Well	Sample	cp	cp/20ul	droplet
A06	DW	-	0	20096
B06	gDNA	10ng	0	20979
C06	Y537N	1000cp	1308	20447
C07	**41m**	**90ng**	0	21512

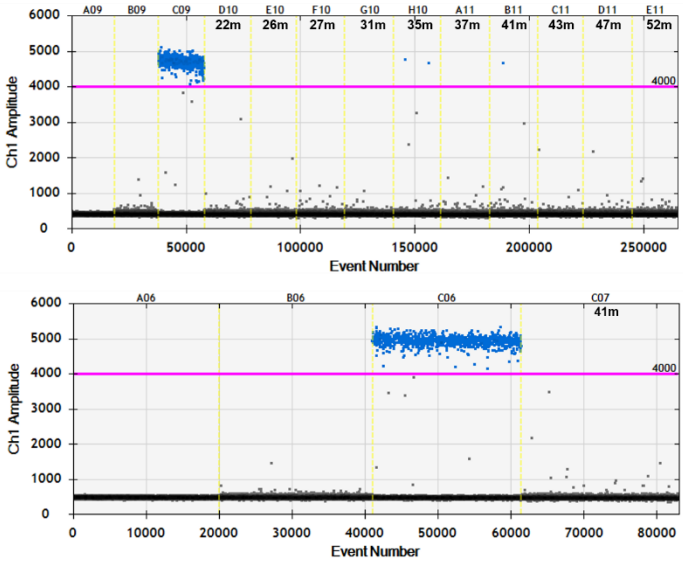

Figure 22. *ESR1* Y537N mutation droplet digital polymerase chain reaction results and plot for the DNAM002 patient.

DW, distilled water.

***ESR1* Y537N – DNAM011**

Well	Sample	cp	cp/20ul	droplet
A01	DW	-	0	20860
B01	gDNA	10ng	0	21035
C01	Y537N	1000cp	1276	19749
E03	**3m**	30ng	3.4	20479
F03	**6m**	30ng	0	13541
G03	**12m**	30ng	0	21586
H03	**17m**	30ng	0	20902
A04	**19m**	30ng	0	20066
B04	**23m**	30ng	0	20714
C04	**26m**	30ng	0	20959
D04	**28m**	30ng	0	21889
E04	**33m**	30ng	0	19705

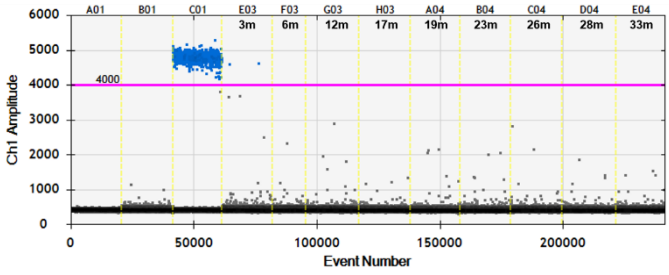

Figure 23. *ESR1* Y537N mutation droplet digital polymerase chain reaction results and plot for the DNAM011 patient.

DW, distilled water.

***ESR1* Y537N – DNAM014**

Well	Sample	cp	cp/20ul	droplet
A01	DW	-	0	20860
B01	gDNA	10ng	0	21035
C01	Y537N	1000cp	1276	19749
F04	**2m**	30ng	0	20851
G04	**6m**	30ng	0	19048
H04	**9m**	30ng	**5.8**	20148

Well	Sample	cp	cp/20ul	droplet
A07	DW	-	0	21866
B07	gDNA	10ng	0	22567
C07	Y537N	1000cp	1288	21641
E07	**14m**	30ng	0	22011
F07	**18m**	30ng	0	21988
G07	**19m**	30ng	0	21759
H07	**21m**	30ng	0	22324
A08	**26m**	30ng	0	21408
B08	**27m**	30ng	0	22081
C08	**34m**	30ng	0	21445
D08	**37m**	30ng	0	21742
E08	**38m**	30ng	0	20677

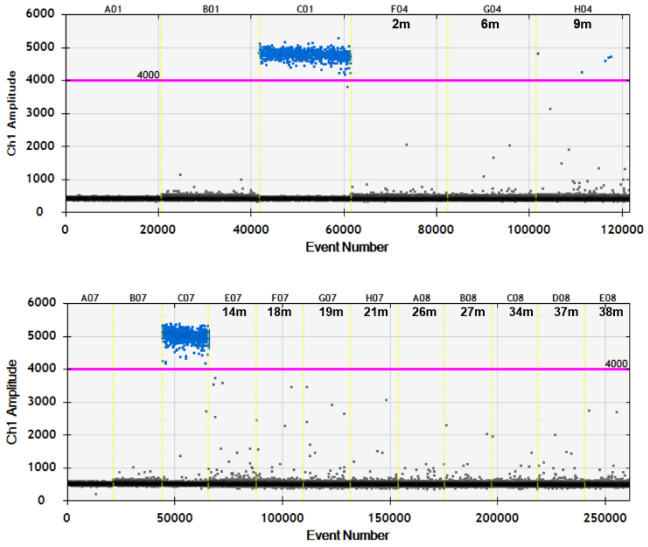

Figure 24. *ESR1* Y537N mutation droplet digital polymerase chain reaction results and plot for the DNAM014 patient.

DW, distilled water.

***ESR1* Y537C – DNAM033**

Well	Sample	cp	cp/20ul	droplet
A01	DW	-	0	20364
B01	gDNA	25ng	0	18962
C01	Y537C	2500cp	0	20453
E01	**5m**	30ng	0	19898
F01	**10m**	30ng	0	19379
G01	**13m**	30ng	0	19429
H01	**15m**	30ng	0	20450
A02	**18m**	30ng	0	15484
B02	**21m**	30ng	**4.6**	15616
C02	**25m**	30ng	**10.4**	15889
D02	**27m**	10ng	**14.8**	15812
E02	**31m**	30ng	**122**	15020

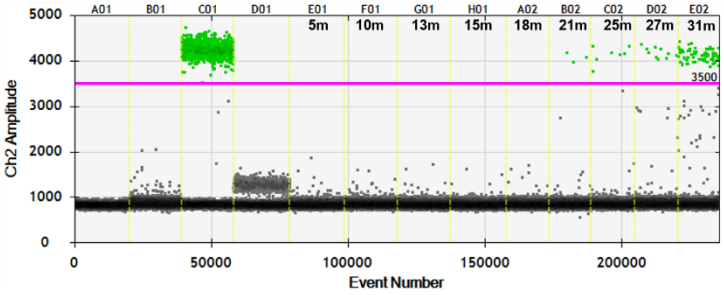

Figure 25. *ESR1* Y537C mutation droplet digital polymerase chain reaction results and plot for the DNAM033 patients.

DW, distilled water.

***ESR1* Y537C – AMCM031**

Well	Sample	cp	cp/20ul	droplet
A09	DW	-	0	21853
B09	gDNA	10ng	0	20271
D09	Y537C	1000cp	958	20541
H09	**32m**	30ng	0	19890
A10	**34m**	30ng	0	21091
B10	**36m**	30ng	0	20549
C10	**38m**	30ng	1.2	20045
D10	**39m**	30ng	0	21078
E10	**43m**	30ng	1.2	21101
F10	**45m**	30ng	0	21131
G10	**47m**	30ng	0	20588
H10	**48m**	30ng	0	20547
A11	**49m**	30ng	0	19790
B11	**50m**	30ng	1	21657
C11	**51m**	30ng	0	20842
D11	**55m**	30ng	0	21198
E11	**56m**	30ng	0	21765
F11	**57m**	30ng	0	21118
G11	**60m**	30ng	0	21303
H11	**62m**	30ng	0	20504

Well	Sample	cp	cp/20ul	droplet
A01	DW	-	0	20426
B01	gDNA	10ng	0	21151
D01	Y537C	1000cp	930	21552
A04	**38m**	**90ng**	0	17273
B04	**43m**	**90ng**	4.2	16967
C04	**50m**	**90ng**	0	16976

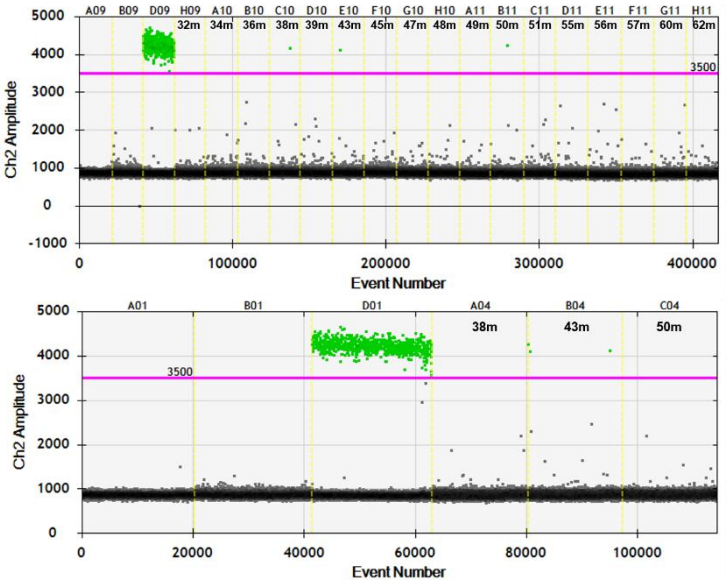

Figure 26. *ESR1* Y537C mutation droplet digital polymerase chain reaction results and plot for the AMCM031 patients.

DW, distilled water.

***ESR1* Y537C – AMCM037**

Well	Sample	cp	cp/20ul	droplet
A09	DW	-	0	21853
B09	gDNA	10ng	0	20271
D09	Y537C	1000cp	958	20541
A12	44m	30ng	1	21534
B12	47m	30ng	0	20512
C12	51m	30ng	0	20533

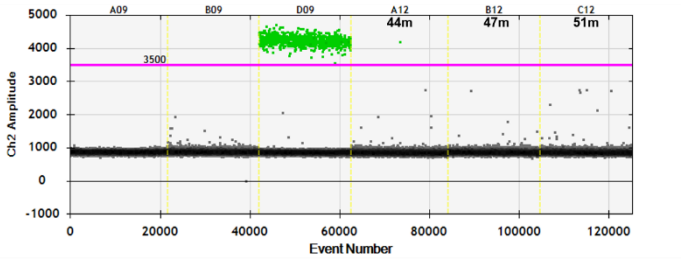

44m sample re-examination

Well	Sample	cp	cp/20ul	droplet
A01	DW	-	0	20426
B01	gDNA	10ng	0	21151
D01	Y537C	1000cp	930	21552
D04	44m	90ng	2.8	16294

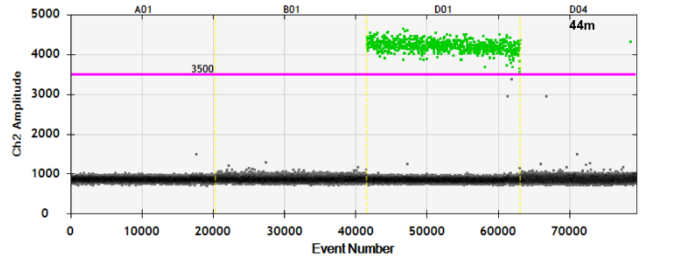

Figure 27. *ESR1* Y537C mutation droplet digital polymerase chain reaction results and plot for the AMCM037 patients.

DW, distilled water.

***ESR1* Y537C – DNAM043**

Well	Sample	cp	cp/20ul	droplet
A09	DW	-	0	21853
B09	gDNA	10ng	0	20271
D09	Y537C	1000cp	958	20541
D12	3m	30ng	0	21178
E12	9m	30ng	0	20099
F12	11m	30ng	0	21158
G12	12m	30ng	0	20567
H12	14m	30ng	1.2	19983

Well	Sample	cp	cp/20ul	droplet
A01	DW	-	0	19195
B01	gDNA	10ng	0	20817
D01	Y537C	1000cp	942	19682
E01	17m	30ng	0	20672
F01	20m	30ng	0	20438
G01	24m	30ng	0	19988
H01	28m	30ng	0	19838
A02	31m	30ng	0	20036
B02	34m	30ng	0	20527
C02	36m	30ng	1.2	20581
D02	40m	30ng	0	18941

14m, 36m sample re-examination

Well	Sample	cp	cp/20ul	droplet
A01	DW	-	0	20426
B01	gDNA	10ng	0	21151
D01	Y537C	1000cp	930	21552
E04	14m	90ng	0	16598
F04	36m	90ng	2.8	16331

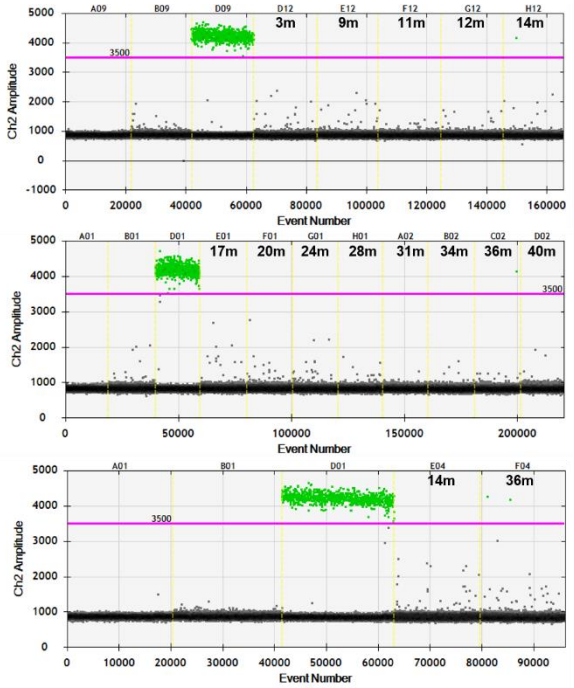

Figure 28. *ESR1* Y537C mutation droplet digital polymerase chain reaction results and plot for the DANM043 patient.

DW, distilled water.

***ESR1* Y537C – DNAM009**

Well	Sample	cp	cp/20ul	droplet
A09	DW	-	0	20274
B09	gDNA	10ng	0	19598
D09	Y537C	1000cp	934	18946
G09	4m	30ng	8	20664
H09	7m	30ng	0	20951
A10	10m	30ng	0	20540
B10	14m	30ng	0	20596
C10	17m	30ng	3.6	19920
D10	19m	30ng	0	20281
E10	21m	30ng	0	20668
F10	23m	30ng	1.2	20097
G10	27m	30ng	1.2	20071
H10	31m	30ng	0	20694
A12	35m	30ng	0	19811
B12	37m	30ng	0	19532
C12	41m	30ng	0	20661
D12	44m	30ng	1.2	20372

23m, 27m, 44m sample re-examination

Well	Sample	cp	cp/20ul	droplet
A06	DW	-	0	18821
B06	gDNA	10ng	0	20075
D06	Y537C	1000cp	942	18998
F07	23m	90ng	0	19906
G07	27m	90ng	0	19549
H07	44m	90ng	0	21588

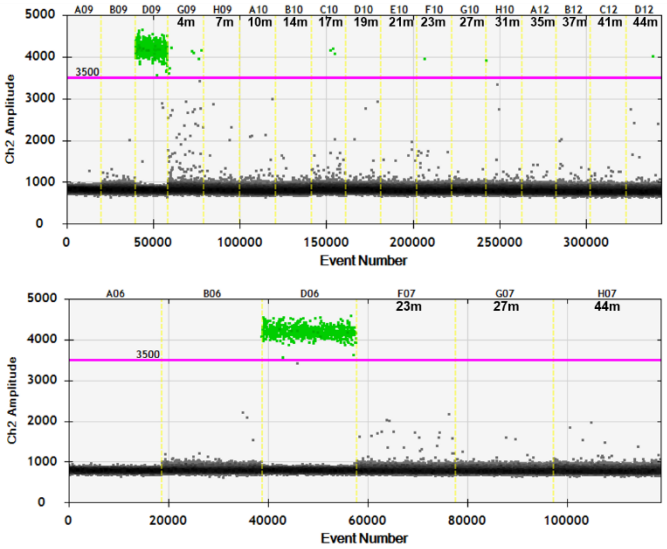

Figure 29. *ESR1* Y537C mutation droplet digital polymerase chain reaction results and plot for the DNAM009 patients.

DW, distilled water.

***ESR1* Y537C – DNAM014**

Well	Sample	cp	cp/20ul	droplet
A09	DW	-	0	20274
B09	gDNA	10ng	0	19598
D09	Y537C	1000cp	934	18946
F11	**2m**	30ng	0	19123
G11	**6m**	30ng	0	17702
H11	**9m**	30ng	0	19563

Well	Sample	cp	cp/20ul	droplet
A01	DW	-	0	21469
B01	gDNA	10ng	0	19899
D01	Y537C	1000cp	888	19347
E01	**14m**	30ng	4.8	19995
F01	**18m**	30ng	0	21079
G01	**19m**	30ng	0	19494
H01	**21m**	30ng	0	20176
A02	**26m**	30ng	0	19717
B02	**27m**	30ng	0	20656
C02	**34m**	30ng	0	21009
D02	**37m**	30ng	0	19203
E02	**38m**	30ng	0	19466

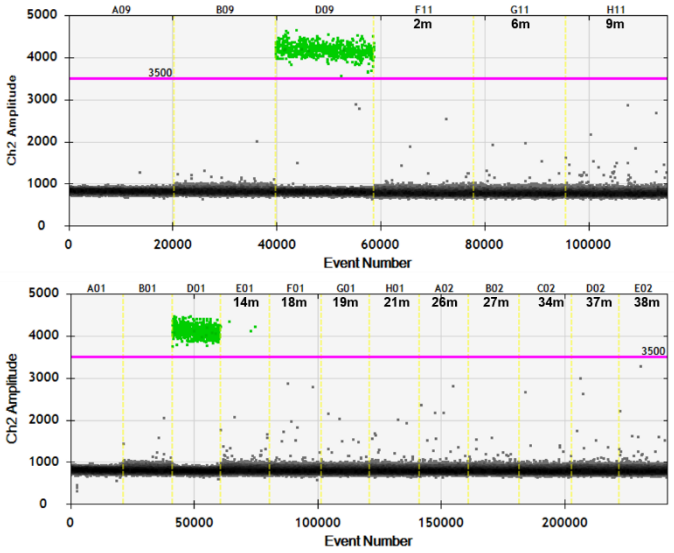

Figure 30. *ESR1* Y537C mutation droplet digital polymerase chain reaction results and plot for the DNAM014 patient.

DW, distilled water.

***ESR1* Y537C – DNAM038**

Well	Sample	cp	cp/20ul	droplet
A01	DW	-	0	21047
B01	gDNA	10ng	0	21613
D01	Y537C	1000cp	990	21741
F01	**3m**	30ng	0	20968
G01	**8m**	30ng	0	21763
H01	**10m**	30ng	0	21099
A02	**14m**	30ng	0	21906
B02	**15m**	30ng	0	21412
C02	**17m**	30ng	0	10254
D02	**21m**	30ng	0	21249
E02	**25m**	30ng	0	21120
F02	**28m**	30ng	1.2	21315
G02	**32m**	30ng	0	22083
H02	**34m**	30ng	1	22139
A03	**38m**	30ng	0	20775
B03	**41m**	30ng	0	21765

28m, 34m sample re-examination

Well	Sample	cp	cp/20ul	droplet
A01	DW	-	0	20426
B01	gDNA	10ng	0	21151
D01	Y537C	1000cp	930	21552
B06	**28m**	90ng	0	20814
C06	**34m**	90ng	2.4	20314

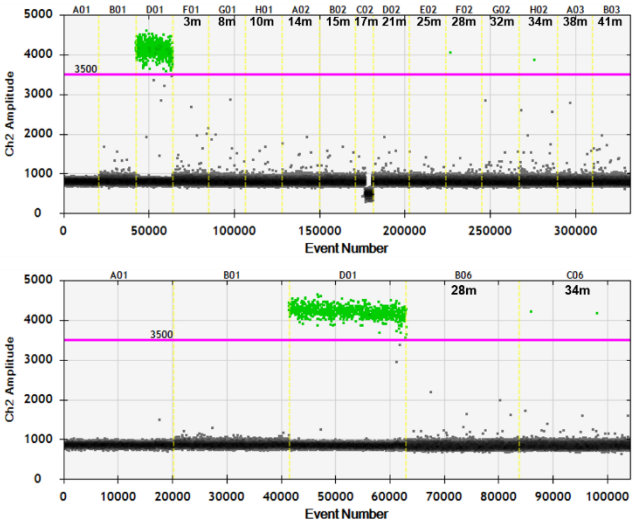

Figure 31. *ESR1* Y537C mutation droplet digital polymerase chain reaction results and plot for the DNAM038 patient.

DW, distilled water.

***ESR1* Y537C – M0005**

Well	Sample	cp	cp/20ul	droplet
A07	DW	-	0	20161
B07	gDNA	10ng	0	19985
D07	Y537C	1000cp	952	19134
G07	**4m**	30ng	0	20105
H07	**6m**	30ng	1.2	20851
A08	**7m**	30ng	0	15576
B08	**10m**	30ng	0	15598
D08	**15m**	30ng	0	15771
E08	**17m**	30ng	0	16389
F08	**23m**	30ng	0	17070
G08	**36m**	30ng	0	17001
H08	**39m**	30ng	0	16977
A09	**42m**	30ng	0	19980
B09	**45m**	30ng	0	19930

Well	Sample	cp	cp/20ul	droplet
A01	DW	-	0	20426
B01	gDNA	10ng	0	21151
D01	Y537C	1000cp	930	21552
G03	**12m**	30ng	0	21223

6m sample re-examination

Well	Sample	cp	cp/20ul	droplet
A01	DW	-	0	20426
B01	gDNA	10ng	0	21151
D01	Y537C	1000cp	930	21552
G03	**6m**	90ng	2.2	20962

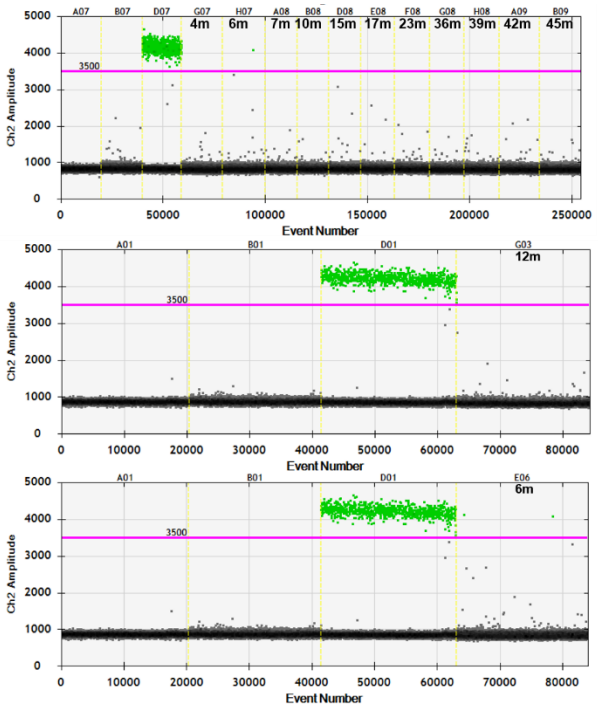

Figure 32. *ESR1* Y537C mutation droplet digital polymerase chain reaction results and plot for the M0005 patient.

DW, distilled water.

***ESR1* Y537S – AMCM027**

Well	Sample	cp	cp/20ul	droplet
A09	DW	-	0	18847
B09	gDNA	10ng	0	20336
C09	Y537S	1000cp	1048	19615
G09	**33m**	30ng	3.4	21116
H09	**35m**	30ng	0	19523
A10	**37m**	30ng	0	19055
B10	**41m**	30ng	0	19364
C10	**43m**	30ng	0	19904

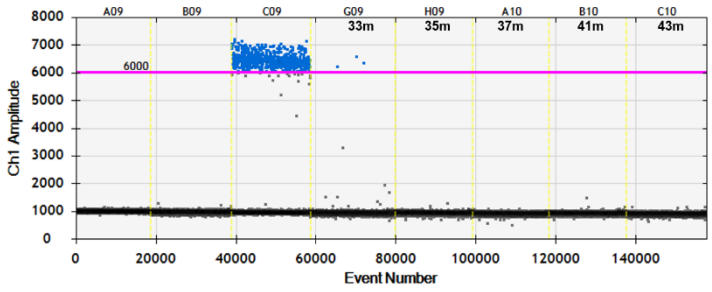

Figure 33. *ESR1* Y537S mutation droplet digital polymerase chain reaction results and plot for the AMCM027 patient.

DW, distilled water.

***ESR1* Y537S – DNAM027**

Well	Sample	cp	cp/20ul	droplet
A09	DW	-	0	21949
B09	gDNA	10ng	0	21379
C09	Y537S	1000cp	1112	20602
G11	**4m**	30ng	0	20683
H11	**8m**	30ng	0	20032
A12	**11m**	30ng	0	20726
B12	**16m**	30ng	0	21851
C12	**19m**	30ng	0	20978
D12	**21m**	30ng	0	21889
E12	**27m**	30ng	0	20250
F12	**29m**	30ng	**2.2**	21615
G12	**32m**	30ng	0	21627
H12	**35m**	30ng	0	19842

Well	Sample	cp	cp/20ul	droplet
A01	DW	-	0	21047
B01	gDNA	10ng	0	21613
C01	Y537S	1000cp	1028	21345
E01	**39m**	30ng	0	21082

29m sample re-examination

Well	Sample	cp	cp/20ul	droplet
A01	DW	-	0	20426
B01	gDNA	10ng	0	21151
C01	Y537S	1000cp	1138	20050
A06	**29m**	**90ng**	**4.4**	21443

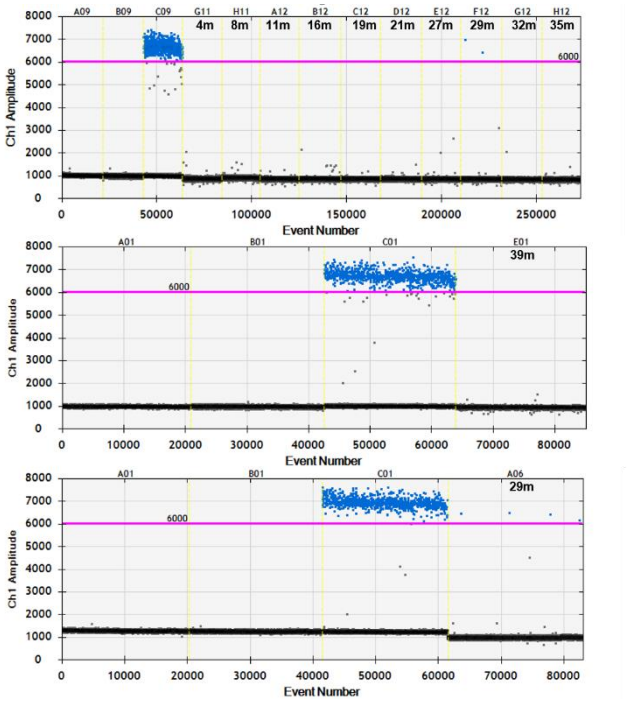

Figure 34. *ESR1* Y537S mutation droplet digital polymerase chain reaction results and plot for the DNAM027 patient.

DW, distilled water.

***ESR1* E380Q – DNAM033**

Well	Sample	cp	cp/20ul	droplet
A05	DW	-	0	22910
B05	gDNA	25ng	0	21770
C05	E380Q	2500cp	3040	22404
E05	**5m**	30ng	0	22595
F05	**10m**	30ng	0	22024
G05	**13m**	30ng	**14.8**	22300
H05	**15m**	30ng	0	21156
A06	**18m**	30ng	0	21201
B06	**21m**	30ng	0	21585
C06	**25m**	30ng	0	21670
D06	**27m**	10ng	0	20416
E06	**31m**	30ng	**2.4**	20434

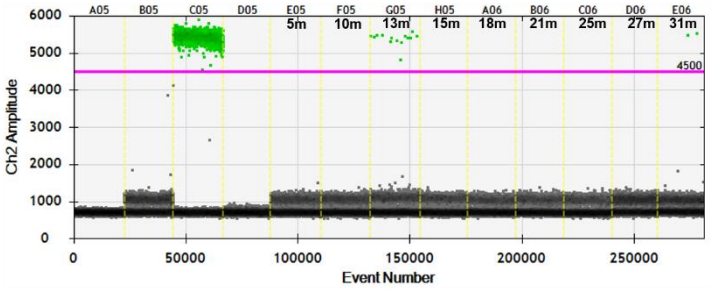

Figure 35. *ESR1* E380Q mutation droplet digital polymerase chain reaction results and plot for the DNAM033 patient.

DW, distilled water.

The clinical course of patients after palliative ETx and *ESR1* mutation detection are shown in Figure 2. Among the patients that were b*ESR1*-positive, eight (50%) showed clinical progression, of which b*ESR1* was detected in four prior to clinical progression. The *ESR1* detection to disease progression times in the DNAM043 patients were 552 and 224 days, while that in the DNAM033 patients were 343 and 119 days. Furthermore, the *ESR1* detection to disease progression time of the DNAM002 patient was 553 days, while that in the AMCM027 was 14 days. In the remaining 4 patients (M005, DNAM024, DNAM014, and DNAM011), mutations were detected simultaneously or after clinical progression. Remarkably, in all patients responding to AI therapy, the b*ESR1* mutation was never detected, or if initially detected, subsequently converted to negative. There were three patients with stable disease in whom the b*ESR1* mutation was never detected.

The clinical course of patients after initiation of ETx and *ESR1* mutation status are depicted in Figure 36. A total of 19 patients received adjuvant ETx with a regimen including tamoxifen. Most of these patients (18/19) subsequently underwent AI-based palliative treatment. Among them, disease progression was observed in 11 patients. b*ESR1* mutations were detected in 7 of the patients in whom the disease progressed. In these patients, b*ESR1* mutation was first detected at 6.0 to 35.1 months after the commencement of palliative AI therapy. Of the two patients who received adjuvant ETx with AI, one (DNAM011) exhibited a b*ESR1* mutation identified 48 months after adjuvant treatment initiation. This patient maintained stable disease for 4 months on palliative fulvestrant before experiencing disease progression.

Figure 36. Swimmer plot showing the *ESR1* mutation status and clinical information of individual patients after initiation of endocrine therapy.

PD, disease progression; OFS, ovarian function suppression; CDK4/6i, cyclin-dependent kinases 4/6 inhibitor.

Patients who received palliative radiotherapy before palliative first-line endocrine therapy were indicated at the start of palliative endocrine therapy.

There were no significant differences in the PFS between patients with b*ESR1* mutation and those without it (p = 0.323; Figure 37). Moreover, a total of three (18.8%) patients with b*ESR1* mutation were detected within 6 months after first-line ETx. They all had distant recurrence with bone-only metastasis; two were treated with CDK4/6i + letrozole, and one was treated with fulvestrant as a palliative first-line ETx. Patients with b*ESR1* mutation within 6 months had a shorter PFS compared to those with b*ESR1* mutation detected after 6 months, although not statistically significant (p = 0.120; median PFS, 5.5 vs. 53.6 months; Figure 38A). Patients with clearance of the b*ESR1* mutation in subsequent cfDNA analyses (81.3%, 13/16) were shown to have a longer PFS than in those where it was detected continuously (p = 0.863; median, PFS 53.6 vs. 42.4 months; Figure 38B). Polyclonality of the b*ESR1* mutation was not significantly associated with PFS (p = 0.393; Figure 38C).

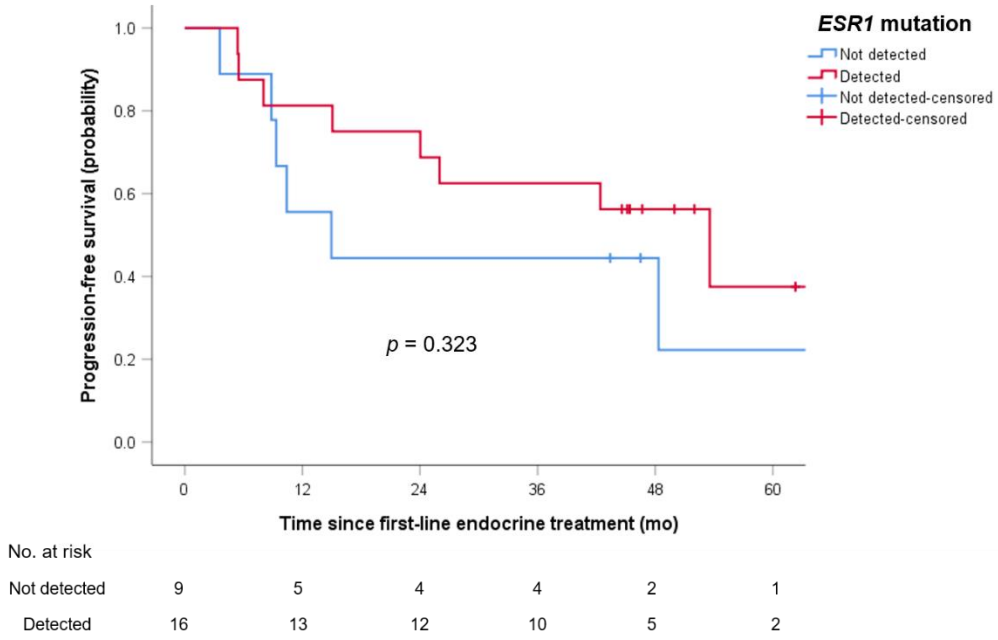

Figure 37. Kaplan–Meier curves of progression-free survival according to *ESR1* mutation status.

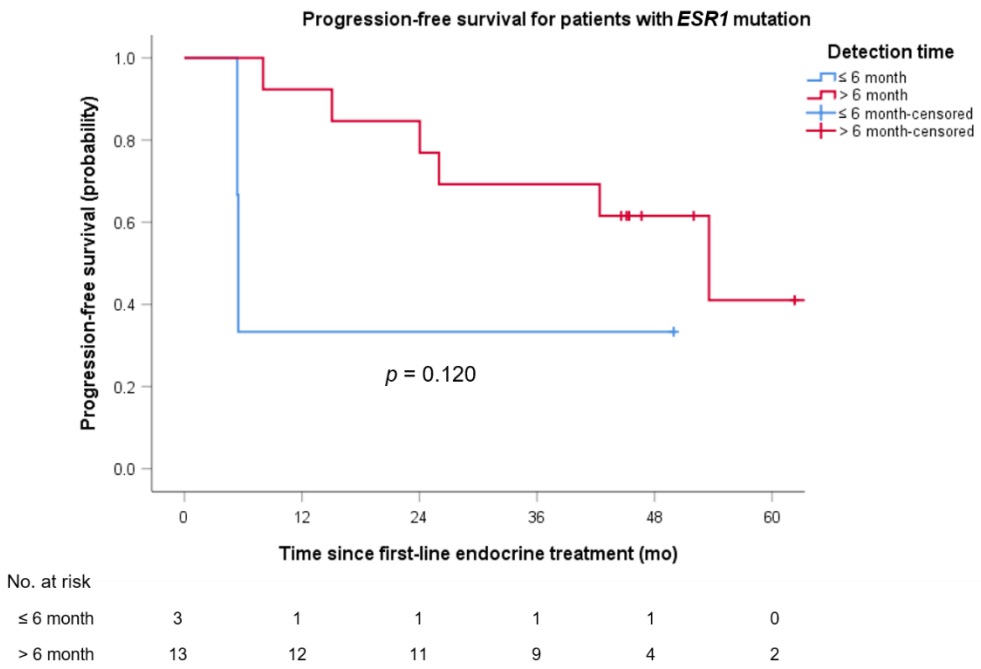

Figure 38A. Kaplan-Meier curves of progression-free survival according to *ESR1* mutation detection time.

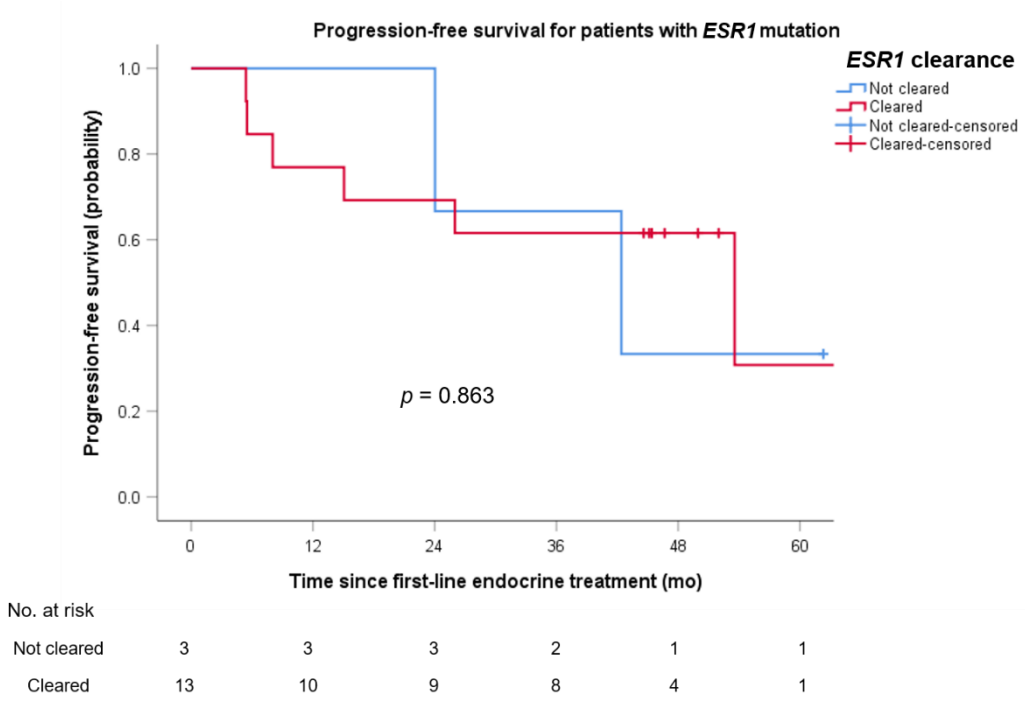

Figure 38B. Kaplan-Meier curves of progression-free survival according to *ESR1* clearance.

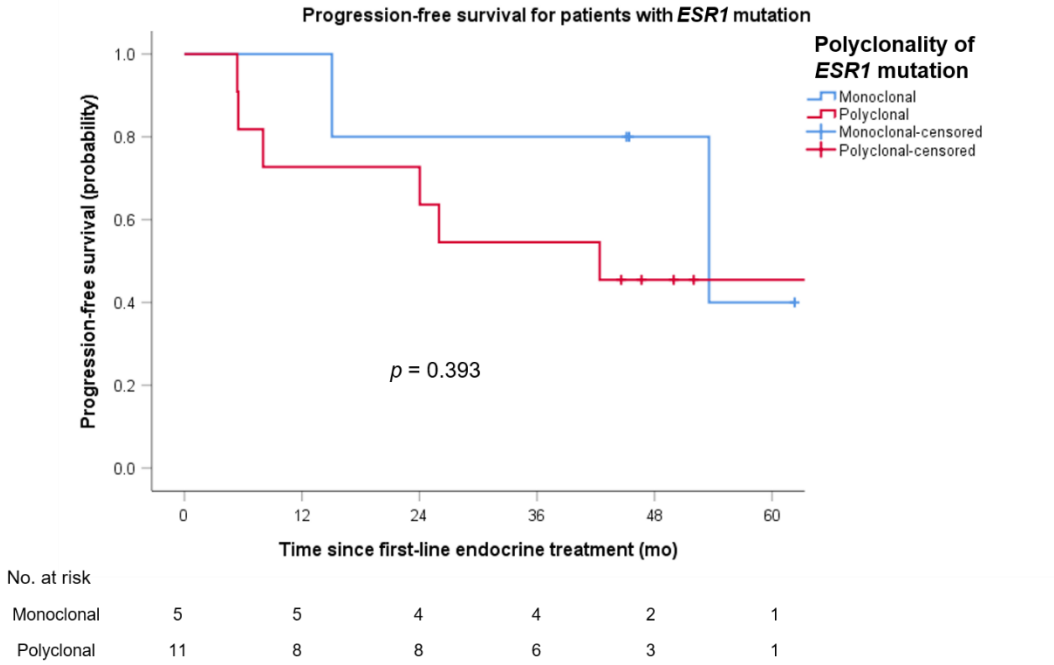

Figure 38C. Kaplan-Meier curves of progression-free survival according to polyclonality of *ESR1* mutations.

Among the 14 patients with clinical progression, eight had b*ESR1* mutations. There were no significant differences in PFS between *ESR1*-mutated and *ESR1*-wild-type patients ($p = 0.457$; Figure 39). The median PFS was 15.1 months (range, 10.2–34.8 months) for patients with b*ESR1* mutation and 9.3 months (range, 2.9–28.9 months) for those without the mutation. Among the patients with disease progression, four died.

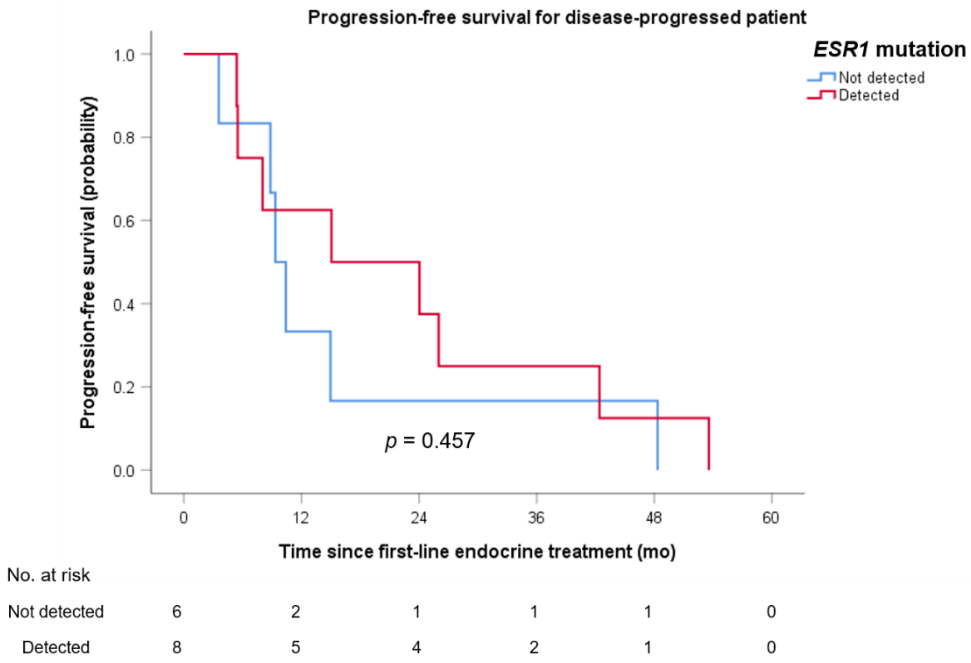

Figure 39. Kaplan–Meier curves of progression-free survival for patients with disease progression according to *ESR1* status.

4.5 *PIK3CA* mutation

The *PIK3CA* mutation analysis was performed in 22 patients using the cfDNA. *PIK3CA* mutations were detected in 68.2% (15/22) of the cfDNA samples at the time of diagnosis of distant metastasis. In primary tumor tissues, *PIK3CA* mutation analysis was performed for 20 patients, of which the mutation was detected in 90.0% (18/20). Using the metastatic tumor tissue, *PIK3CA* mutation analysis was performed on seven patients, among whom the mutation was detected in 57.1% (3/7). The *PIK3CA* mutation results for each patient and sample, with variant allele frequencies (VAF), are shown in Figure 40. Most *PIK3CA* mutations detected in the primary tumor tissue showed low VAF values when detected in the plasma. Heterogeneity was observed between the mutational types for each sample. In four patients, *PIK3CA* mutations were detected in the primary tumor tissue but not in cfDNA (AMCM037, AMCM031, DNAM009, and DNAM017). When the *PIK3CA* mutation was detected in primary tumor tissue but not in plasma, the interval between tissue sampling tended to be longer (64.0 months vs. 79.2 months, $p = 0.230$). The intervals for tissue and plasma sampling of these patients were 193.7, 67.7, 24.1, and 31.2 months, respectively. The VAF values in the primary tumor tissues of these discordant patients ranged from 0.98 to 14.91 for AMCM037, 1.14 to 3.01 for AMCM031, 3.48 for DNAM009, and 1.11 to 1.17 for DNAM017. In contrast, *PIK3CA* mutations were detected in the cfDNA but not in the primary tumor tissue in just one patient (DNAM051). The interval between tissue and plasma sampling for this patient was 10.3 months. The most frequent *PIK3CA* mutations were H1047R (25.4%), E545K (19.5%), H1047Y (12.7%), E542K (12.7%), and H1047L (10.2%).

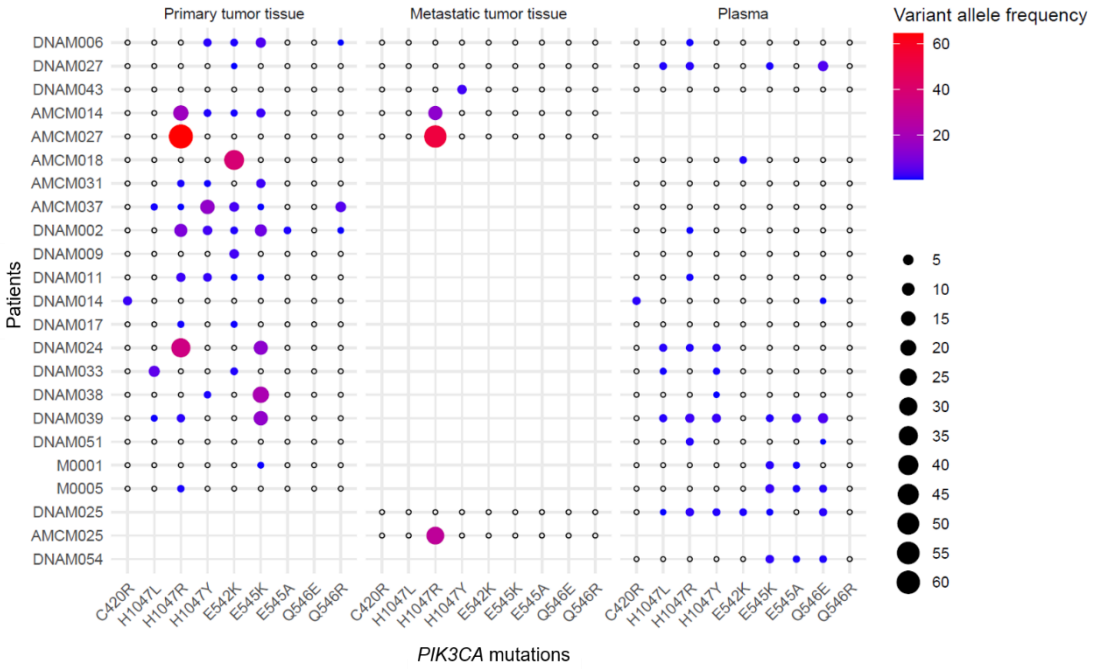

Figure 40. *PIK3CA* mutation status.

Patients with a blood *PIK3CA* mutation at the time of diagnosis of metastasis presented with a significantly shorter PFS (p = 0.024) than those without mutations (Figure 41A). The presence of *PIK3CA* mutations in the primary tumor tissue was not significantly associated with PFS (p = 0.428; Figure 41B) or DFS (p = 0.716; Figure 41C). Patients with *PIK3CA* mutations in metastatic tumor tissue had a shorter PFS compared to those without, although the difference was not statistically significant (p = 0.093; Figure 41D).

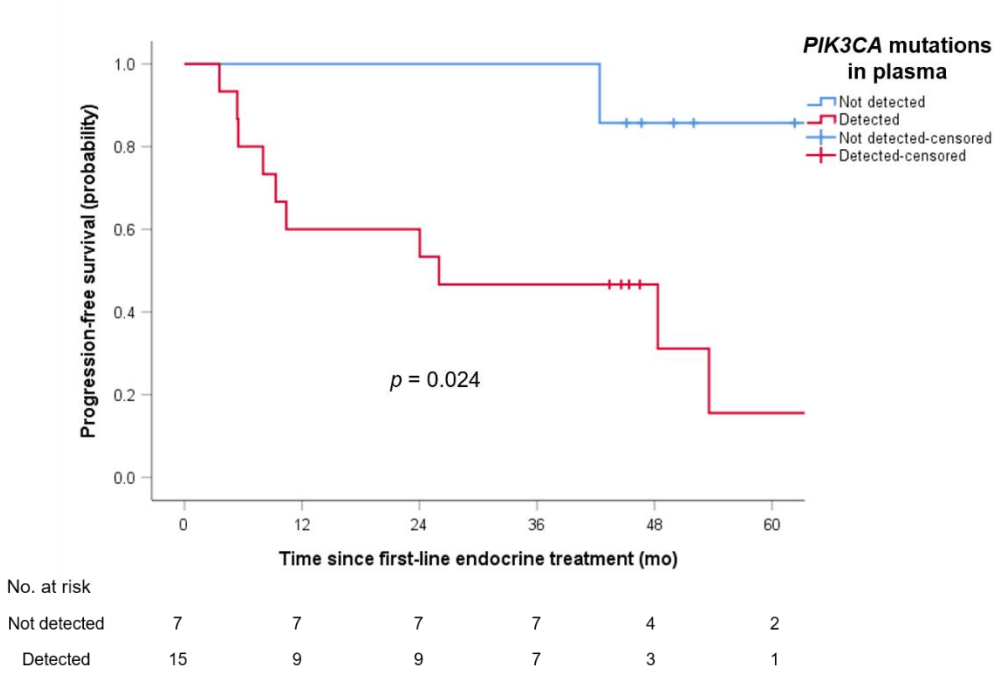

Figure 41A. Kaplan–Meier curves of progression-free survival according to *PIK3CA* mutations in plasma.

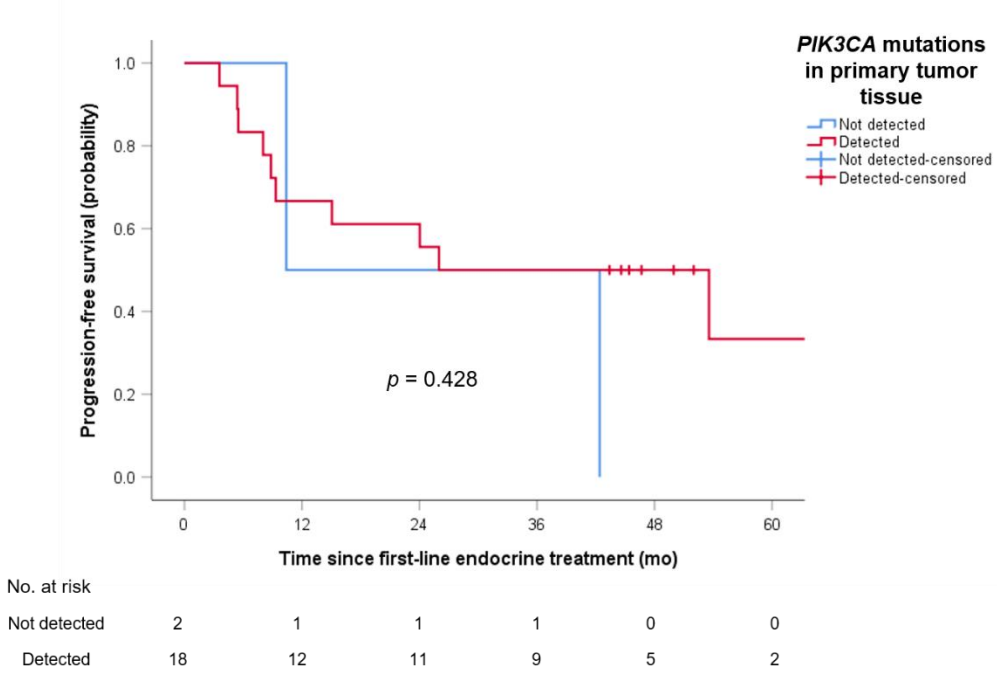

Figure 41B. Kaplan–Meier curves of progression-free survival according to *PIK3CA* mutations in primary tumor tissue.

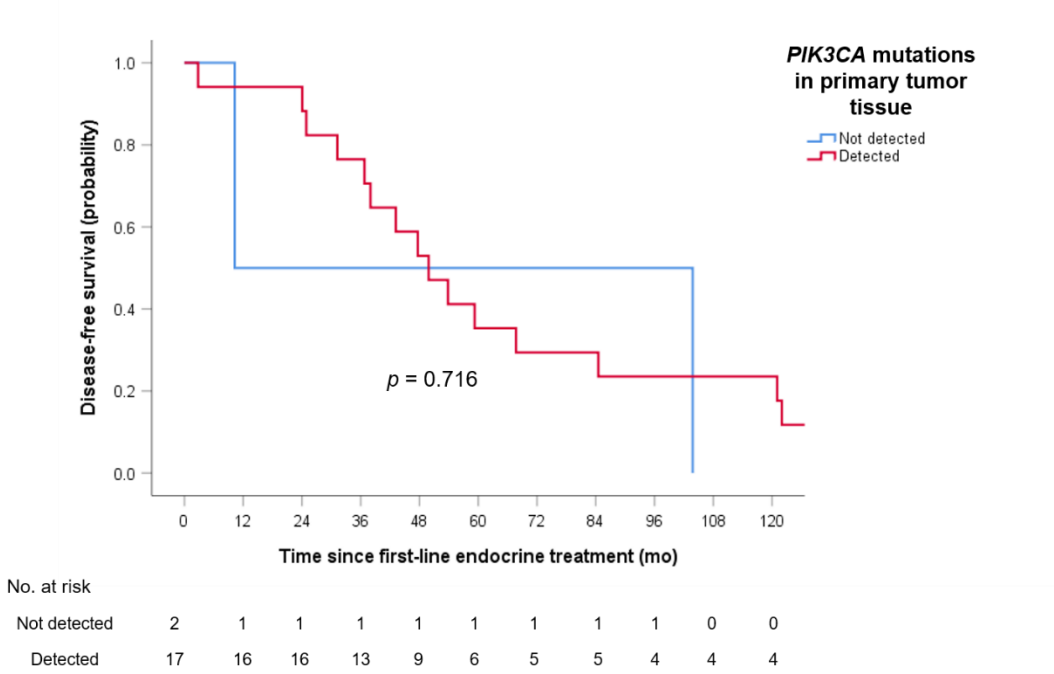

Figure 41C. Kaplan–Meier curves of disease-free survival according to *PIK3CA* mutations in primary tumor tissue.

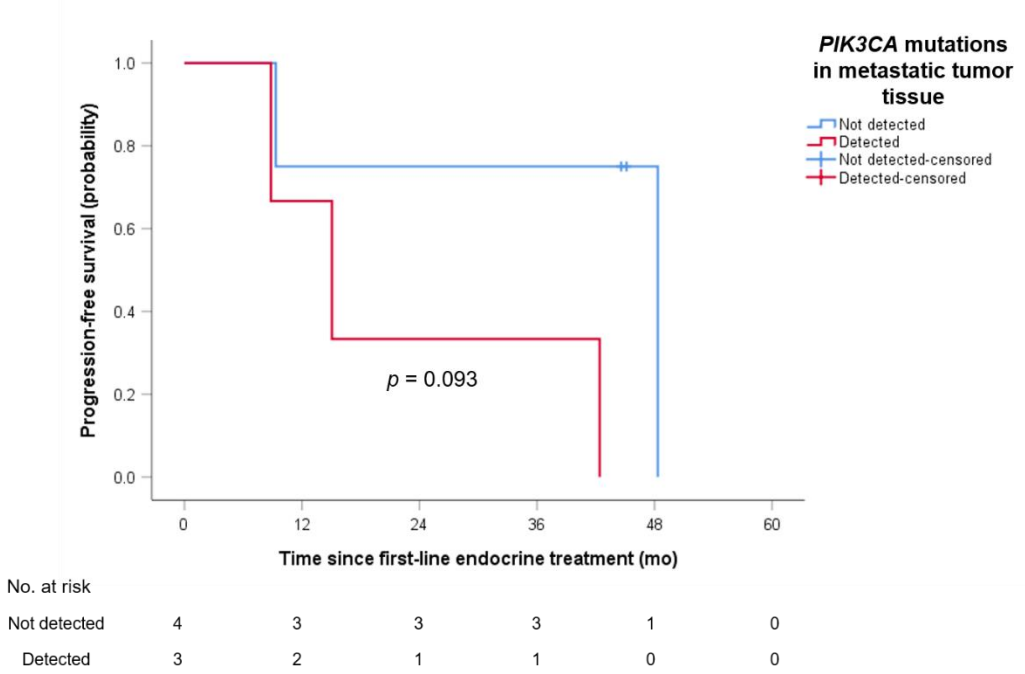

Figure 41D. Kaplan–Meier curves of progression-free survival according to *PIK3CA* mutations in metastatic tumor tissue.

4.6 *ESR1* and *PIK3CA* mutations

In patients with *PIK3CA* mutations in the plasma, 53.3% (8/15) also had b*ESR1* mutations. Patients with both b*ESR1* and *PIK3CA* mutations showed shorter PFS with marginal significance ($p = 0.057$; Figure 42).

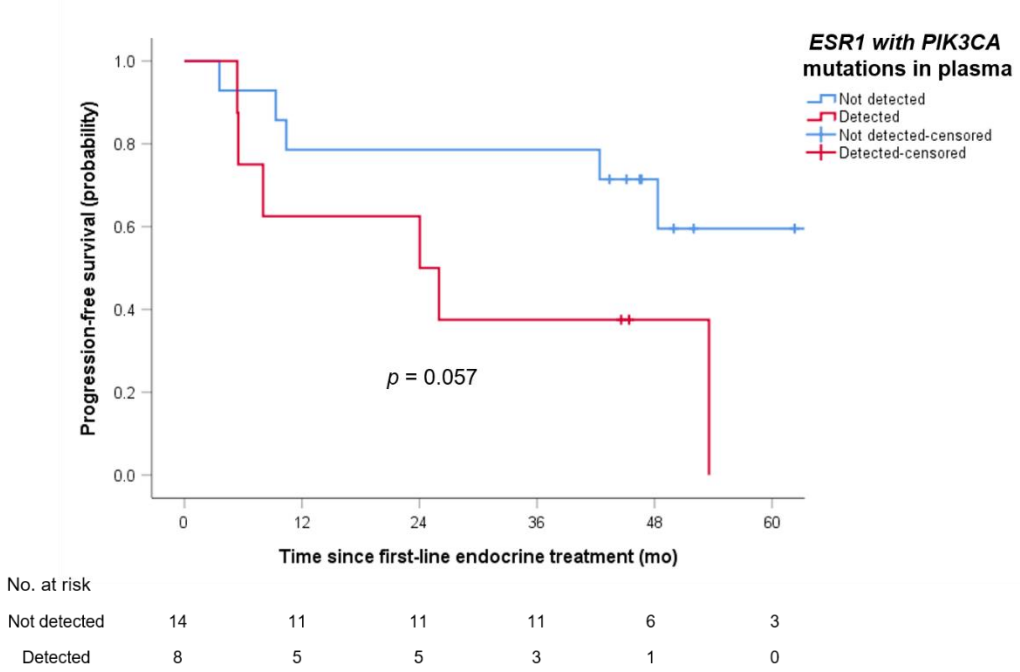

Figure 42. Kaplan–Meier curves of progression-free survival according to the co-occurrence of *ESR1* and *PIK3CA* mutations in plasma.

Representative examples of serial changes in *ESR1* mutations with available *PIK3A* mutations result in the cfDNA during the clinical course are shown in Figures 43–46. In patient DNAM033, *PIK3CA* mutations were detected in the plasma at the time of distant metastasis. The *ESR1* E380Q mutation was detected and eliminated; however, the disease progressed after the Y537C mutation gradually increased (Figure 43). Patient DNAM043 did not have *PIK3CA* mutation; however, the *ESR1* Y537N mutation copy number increased before disease progression (Figure 44). Patient DNAM014 had *PIK3CA* mutations, and several types of *ESR1* mutations were detected at the time of disease progression. However, all *ESR1* mutations were cleared after second-line treatment. However, the disease progressed after 23 months (Figure 45). In patients DNAM027, there were *PIK3CA* mutations, and *ESR1* mutations also appeared during ETx but were cleared and remained in a stable disease state (Figure 46).

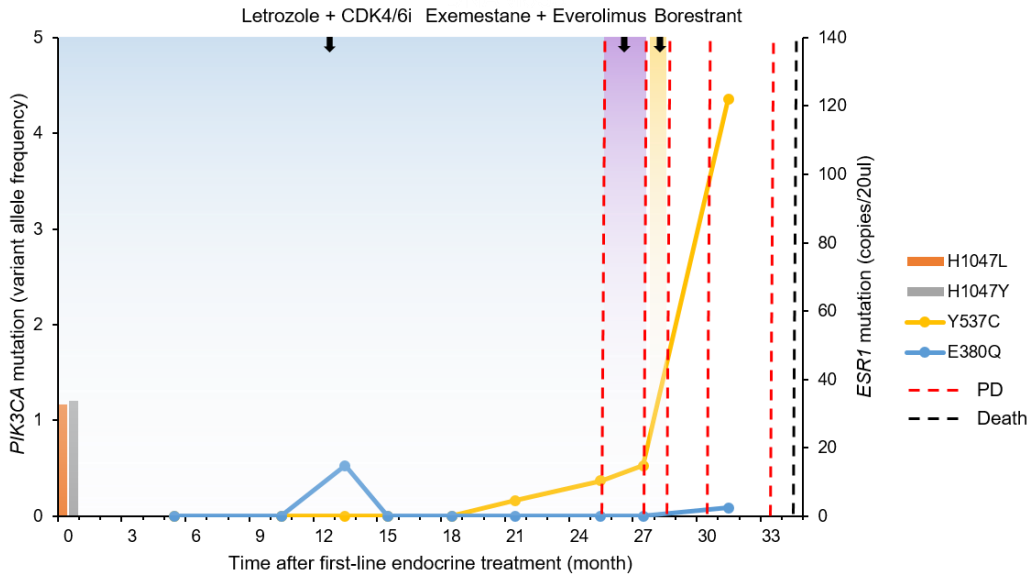

Figure 43. ctDNA trajectories in patient DNAM033.

CDK4/6i, cyclin-dependent kinases 4/6 inhibitor; PD, disease progression.

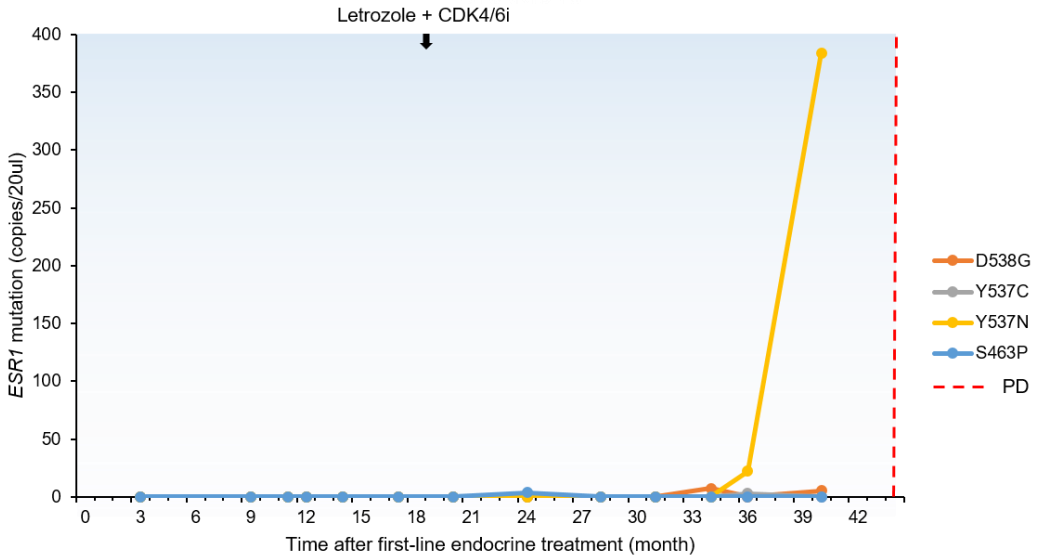

Figure 44. ctDNA trajectories in patient DNAM043.

CDK4/6i, cyclin-dependent kinases 4/6 inhibitor; PD, disease progression.

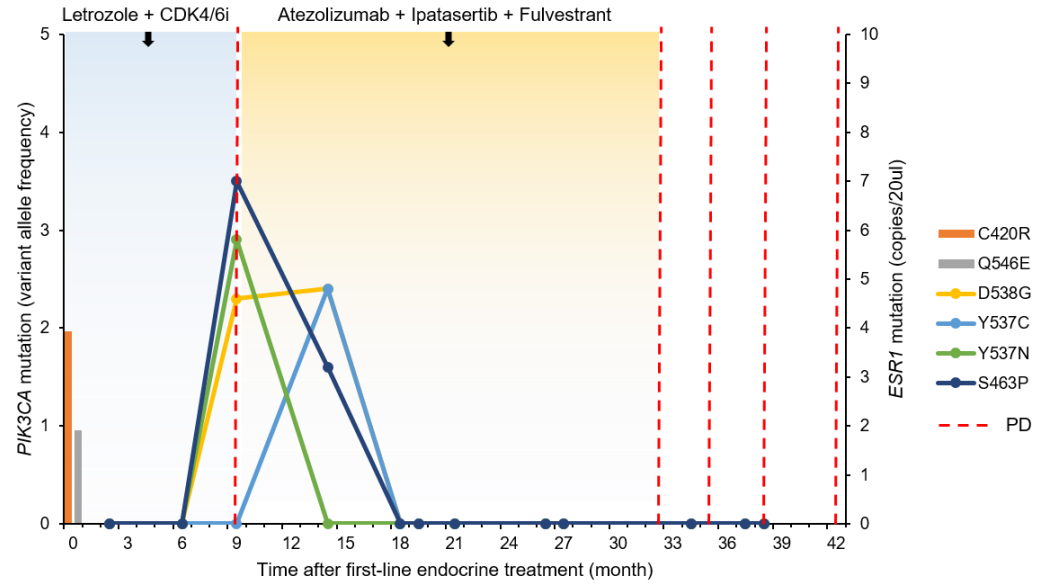

Figure 45. ctDNA trajectories in patient DNAM014.

CDK4/6i, cyclin-dependent kinases 4/6 inhibitor; PD, disease progression.

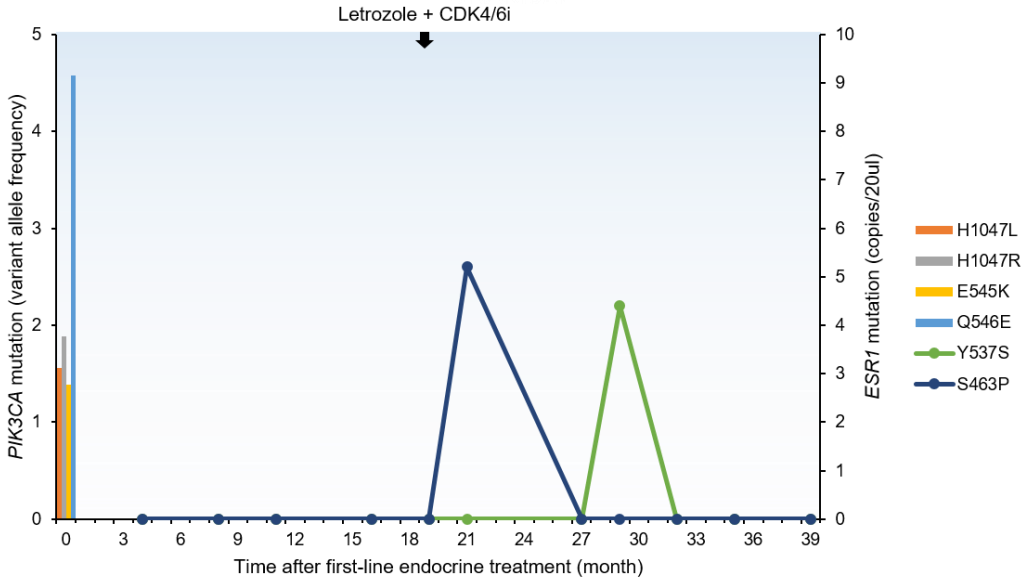

Figure 46. ctDNA trajectories in patient DNAM027.

CDK4/6i, cyclin-dependent kinases 4/6 inhibitor.

In all patients with primary endocrine resistance (DNAM051 and DNAM039), no *ESR1* mutation was found (Figure 36), but a plasma *PIK3CA* mutation was detected. Among the 20 patients with secondary endocrine resistance, *ESR1* mutations were detected in 70%, and plasma *PIK3CA* mutations were detected in 60%. Furthermore, *ESR1* mutations were detected in 2 out of 3 patients with endocrine-sensitive *de novo* metastasis (M0008, DNAM054, and AMCM007; Figure 2), and a plasma *PIK3CA* mutation was detected in 1 patient.

5. Discussion

In this longitudinal ctDNA analysis of patients with metastatic HR-positive/HER2-negative breast cancer during first-line ETx, we reported the prevalence and clinical course of *ESR1* and *PIK3CA* mutations and analyzed their correlation with PFS. *ESR1* and *PIK3CA* mutations were detected in 64.0% and 68.2% of plasma samples, respectively. Half of the patients with b*ESR1* mutations showed clinical progression after palliative first-line ETx. The presence of *PIK3CA* mutations in cfDNA significantly affected the PFS.

We investigated the serial changes in *ESR1* mutations in the cfDNA during palliative treatment using individual case reviews. Some patients showed disease progression with a gradual increase in *ESR1* mutations (Figures 43 and 44). One patient had a cleared mutation after treatment, and it can be assumed that the subsequent disease progression was caused by other resistance mechanisms (Figure 45). The initial disease progression in this patient was estimated to be driven by an *ESR1* mutation. However, despite the disappearance of *ESR1* mutation clones following a change in the ETx regimen, progression still occurred. If no known hotspot mutations are identified at this stage, it may be necessary to detect other newly acquired mutations using different panel testings. Since b*ESR1* mutations were confirmed early in these patients, or at least at the time of clinical progression, monitoring responses with serial blood tests could be advantageous, particularly if the mutations targeted during ETx for these tumors are clearly identified. Additionally, there was a case responding to ETx even though several types of *ESR1* mutations were detected intermittently (Figure 46). These findings confirm that *ESR1* mutations change dynamically during treatment and can be of various types. In cases where b*ESR1* mutations were detected but the disease remained stable, follow-up samples showed negative conversion. It is currently unclear how many negative tests or months of confirmation are to ensure that this does not lead to clinical disease progression. In the PADA-1 study, some patients had a rising *ESR1* mutation but did

not change their ETx regimen and remained progression-free (36). Although their serial *ESR1* data has not been released yet, it is thought that such a population will probably show a similar pattern as our study. Previous studies also reported that *ESR1* mutation status changes during treatment (38, 39). This suggests that interpretation should be made as a comprehensive course for each patient through serial follow-ups rather than by detecting ctDNA at a specific time point.

The prevalence of *ESR1* mutations was 64.0% in this study, which was higher than that reported in previous studies with various patient and treatment profiles (10, 13, 14, 16, 36). This may be because our study included many patients who received AIs (88.0%) for metastasis. Schiavon et al. reported that *ESR1* mutations were present at a higher rate in patients treated with AIs in a metastatic setting and rarely in patients treated with AIs in an adjuvant setting (13). Additionally, many patients with bone metastases were included in this study. Fifteen (60.0%) patients had bone metastases, 11 patients had bone-only metastases, and 4 had bone metastases with other metastatic sites. Fribbens et al. reported that *ESR1* mutations are significantly associated with bone metastasis (16).

PIK3CA mutations were detected in 68.2% of the patients. The frequency of *PIK3CA* mutations in ctDNA from patients with metastatic breast cancer varies between studies (22-25) but was found to be slightly higher in our study. A high concordance rate between *PIK3CA* mutations in primary tumor tissues and ctDNA has been reported (24, 25). Most (90.0%) patients included in our study with available *PIK3CA* test data had *PIK3CA* mutations in the primary tumor tissue and, therefore, also in ctDNA at a high prevalence. In our study, *PIK3CA* mutations were found in 90% of the primary tumor tissues, which was higher than that reported in previous studies reporting *PIK3CA* mutations in archived tumor tissues (24, 25, 40). Although the prevalence by mutation type showed similar results to those of previous studies for other mutation types (41), the proportion of the H1047Y

mutation was higher, which is a known rare mutation. Additional studies are planned to determine whether the discrepancy in mutation type incidence was due to selection bias in the patient group, heterogeneous treatment profiles, or differences in mutation detection assays.

Regarding the clinical course of patients, 50% of the patients with b*ESR1* mutations showed clinical progression, of which four had b*ESR1* detected before clinical progression. There were also cases where b*ESR1* was detected simultaneously with clinical progression and slightly later, suggesting the necessity for closer intervals for cfDNA analyses. This finding also suggests that the detection of mutations in ctDNA may be a potential substitute for routine radiological tests. Previous studies have shown the possibility of the early detection of ctDNA before disease progression (42-44). However, there were patients whose blood samples were collected simultaneously or later than in the radiological study. Owing to the nature of the patient cohort included in this study, blood samples were mainly collected along with the patients' radiological or blood test schedules, and there was no time point when blood sampling was substituted for radiologic tests. Therefore, it was difficult to clearly determine whether mutations were first detected in ctDNA or whether progression in radiological study occurred first. Further prospective trials are needed to determine the time order between ctDNA detection and clinical progression and to estimate the lead time. Meanwhile, six patients progressed, even though b*ESR1* mutations were not detected in the ctDNA (Figure 2). Although a significant proportion of cases with endocrine resistance are associated with *ESR1* mutations, other resistance mechanisms that are mutually exclusive to *ESR1* have also been identified (45). It can be assumed that other resistance mechanisms may have contributed to the disease progression in these patients.

Early and sustained detection of mutations in ctDNA tended to result in shorter PFS, although this was not statistically significant. Polyclonality of the b*ESR1* mutation was not

associated with PFS, which is consistent with previous studies (16, 39). In our study, the b*ESR1* mutation was not significantly associated with PFS. However, *ESR1* mutations are considered to be associated with poor PFS (46, 47). Because the number of patients tested was small, it was difficult to confirm the impact of b*ESR1* mutations on PFS. Further studies are needed to confirm the impact of b*ESR1* mutation on PFS through prospective studies with large numbers of patients. We performed a retrospective analysis of a prospectively collected sample, and no intervention was performed on the patient when a b*ESR1* mutation was detected in the ctDNA. In the PADA-1 trial, there was a PFS benefit for the early switch of ETx before clinical relapse through serial ctDNA monitoring of rising b*ESR1* mutations (36). This finding suggests the need for serial monitoring of ctDNA during ETx and early intervention.

ESR1 mutation is an acquired mutation after ETx as a result of therapeutic pressure. Most clinical trials on ETx enrolled patients who received first-line treatment for at least six months; therefore, *ESR1* mutation testing was also performed six months after first-line ETx. (19, 48). However, our study examined blood samples collected within 6 months of starting palliative ETx and revealed that patients who developed *ESR1* mutations within 6 months of palliative ETx tended to have a shorter PFS. These results highlight the need for early ctDNA monitoring, which should be considered in future clinical trials.

In this study, among patients with disease progression, patients with b*ESR1* mutations exhibited numerically longer PFS than those without the mutation (15.1 months vs. 9.3 months, $p = 0.457$). Razavi et al. identified mitogen-activated protein kinase mutations that were mutually exclusive of *ESR1* mutations associated with a shorter response duration to subsequent ETx (45). Previous studies have also identified multiple genomic alterations that are associated with poor outcome in HR-positive/HER2-negative metastatic breast cancer (49, 50). This result suggests that there may be limitations to treatments based on *ESR1*

mutation status alone because other driver mutations may have a more negative impact on therapeutic resistance. Future research should be conducted to reveal the relationship between *ESR1* and other mutations and their impact on treatment outcomes.

The SOLAR-1 trial demonstrated PFS benefit for those treated with alpelisib, an oral PI3K-α-specific inhibitor, with fulvestrant among patients with *PIK3CA*-mutated/HR-positive/HER2-negative advanced breast cancer who had previously received ETx (27). Therefore, this mutation should be identified, and targeted therapy should be considered for metastatic HR-positive/HER2-negative breast cancer. In the SOLAR-1 trial, *PIK3CA* status was evaluated in a tumor tissue sample, preferably in the sample obtained during the most recent progression (27). In our study, the detection of blood *PIK3CA* mutations at the time of metastasis diagnosis was associated with significantly shorter PFS, but the primary tumor tissue was not. The reason why the primary tumor tissue was found to be unrelated to the PFS outcome may be that very few patients included in the study did not have a *PIK3CA* mutation. The co-occurrence of b*ESR1* and blood *PIK3CA* mutations was also associated with shorter PFS. These findings suggest that identifying *PIK3CA* mutations using cfDNA could also benefit from targeted treatments.

The use of cfDNA testing in patients with cancer has been highlighted as the sensitivity and accuracy of the technology improve for detecting rare mutant variants (51). Using ddPCR and an amplicon-based targeted NGS method, we detected *ESR1* and *PIK3CA* mutations at rates comparable to those reported in previous studies. ddPCR enables the detection of a 0.001% mutant fraction (52). Amplicon-based targeted NGS can amplify and sequence large genomic regions from a single ctDNA copy (53). In the present study, we confirmed that these methods are reliable for the detection of mutations. cfDNA is a minimally invasive assay for detecting *ESR1* and *PIK3CA* mutations. Optimization of these tests will lead to personalized and precision medicine.

This study had several limitations. First, this study involves a small number of patients, limiting its statistical relevance. Nevertheless, we found that patients with *PIK3CA* mutations presented significantly worse PFS and found a trend toward worse PFS with early detection of b*ESR1*, clearance of b*ESR1*, and the co-occurrence of *ESR1* and *PIK3CA* mutations. These findings highlight the need for identifying these mutations during ETx. Second, this study was a retrospective analysis of prospectively collected samples and was not randomized. Therefore, there may have been selection bias. However, in this study, we aimed to show the clinical results in a real-world setting. Finally, only *ESR1* and *PIK3CA* mutations were identified. However, as other resistance mechanisms may have contributed to disease progression, there are limitations in interpreting the clinical course of each patient based solely on these results.

Our study had the strength of sequentially following each patient with samples from multiple time points during palliative treatment. Previous studies that examined b*ESR1* mutations in metastatic breast cancer samples at limited time points were limited in showing *ESR1* mutation dynamics during the treatment period. (38, 54). Our results will help us understand the development of resistance and disease progression during ETx in clinical practice. In addition, in the real world, there are cases where CDK4/6i cannot be used and disparities in its use exist (55). Our study included patients who had not been treated with the current standard ETx for various reasons, showing the actual mutation results of patients who received various ETx.

In conclusion, a substantial number of patients with HR-positive/HER2-negative metastatic breast cancer were found to harbor *ESR1* or *PIK3CA* mutations in serial plasma samples. Early detection of b*ESR1* within 6 months of palliative ETx and sustained b*ESR1* during palliative ETx were associated with a trend toward shorter PFS. The co-occurrence of b*ESR1* and blood *PIK3CA* mutations was associated with a shorter PFS with marginal significance.

PIK3CA mutations in cfDNA are prognostic factors, suggesting the benefit of combined targeted therapies for these mutations.

6. References

1. Giaquinto AN, Sung H, Miller KD, Kramer JL, Newman LA, Minihan A, et al. Breast Cancer Statistics, 2022. CA Cancer J Clin. 2022;72(6):524-41.

2. Osborne CK. Tamoxifen in the treatment of breast cancer. N Engl J Med. 1998;339(22):1609-18.

3. Goss PE, Strasser K. Aromatase inhibitors in the treatment and prevention of breast cancer. J Clin Oncol. 2001;19(3):881-94.

4. Howell A, Osborne CK, Morris C, Wakeling AE. ICI 182,780 (Faslodex): development of a novel, "pure" antiestrogen. Cancer. 2000;89(4):817-25.

5. Early Breast Cancer Trialists' Collaborative Group (EBCTCG); Davies C, Godwin J, Gray R, Clarke M, Cutter D, Darby S, et al. Relevance of breast cancer hormone receptors and other factors to the efficacy of adjuvant tamoxifen: patient-level meta-analysis of randomised trials. Lancet. 2011;378(9793):771-84.

6. Pan H, Gray R, Braybrooke J, Davies C, Taylor C, McGale P, et al. 20-Year Risks of Breast-Cancer Recurrence after Stopping Endocrine Therapy at 5 Years. N Engl J Med. 2017;377(19):1836-46.

7. Rasha F, Sharma M, Pruitt K. Mechanisms of endocrine therapy resistance in breast cancer. Mol Cell Endocrinol. 2021;532:111322.

8. Aleskandarany MA, Rakha EA, Ahmed MAH, Powe DG, Paish EC, Macmillan RD, et al. PIK3CA expression in invasive breast cancer: a biomarker of poor prognosis. Breast Cancer Res Treat. 2010;122(1):45-53.

9. Chandarlapaty S, Chen D, He W, Sung P, Samoila A, You D, et al. Prevalence of *ESR1* Mutations in Cell-Free DNA and Outcomes in Metastatic Breast Cancer: A Secondary Analysis of the BOLERO-2 Clinical Trial. JAMA Oncol. 2016;2(10):1310-5.

10. Zundelevich A, Dadiani M, Kahana-Edwin S, Itay A, Sella T, Gadot M, et al. *ESR1* mutations are frequent in newly diagnosed metastatic and loco-regional recurrence of endocrine-treated breast cancer and carry worse prognosis. Breast Cancer Res. 2020;22(1):16.

11. Lei JT, Gou X, Seker S, Ellis MJ. *ESR1* alterations and metastasis in estrogen receptor positive breast cancer. J Cancer Metastasis Treat. 2019;5.

12. Fanning SW, Mayne CG, Dharmarajan V, Carlson KE, Martin TA, Novick SJ, et al. Estrogen receptor alpha somatic mutations Y537S and D538G confer breast cancer endocrine resistance by stabilizing the activating function-2 binding conformation. Elife. 2016;5.

13. Schiavon G, Hrebien S, Garcia-Murillas I, Cutts RJ, Pearson A, Tarazona N, et al. Analysis of *ESR1* mutation in circulating tumor DNA demonstrates evolution during therapy for metastatic breast cancer. Sci Transl Med. 2015;7(313):313ra182.

14. Wang P, Bahreini A, Gyanchandani R, Lucas PC, Hartmaier RJ, Watters RJ, et al. Sensitive Detection of Mono- and Polyclonal ESR1 Mutations in Primary Tumors, Metastatic Lesions, and Cell-Free DNA of Breast Cancer Patients. Clin Cancer Res. 2016;22(5):1130-7.

15. Weis KE, Ekena K, Thomas JA, Lazennec G, Katzenellenbogen BS. Constitutively active human estrogen receptors containing amino acid substitutions for tyrosine 537 in the receptor protein. Mol Endocrinol. 1996;10(11):1388-98.

16. Fribbens C, O'Leary B, Kilburn L, Hrebien S, Garcia-Murillas I, Beaney M, et al. Plasma *ESR1* Mutations and the Treatment of Estrogen Receptor-Positive Advanced Breast Cancer. J Clin Oncol. 2016;34(25):2961-8.

17. Toy W, Weir H, Razavi P, Lawson M, Goeppert AU, Mazzola AM, et al. Activating *ESR1* Mutations Differentially Affect the Efficacy of ER Antagonists. Cancer Discov. 2017;7(3):277-87.

18. Bidard FC, Kaklamani VG, Neven P, Streich G, Montero AJ, Forget F, et al. Elacestrant (oral selective estrogen receptor degrader) Versus Standard Endocrine Therapy for Estrogen Receptor-Positive, Human Epidermal Growth Factor Receptor 2-Negative Advanced Breast Cancer: Results From the Randomized Phase III EMERALD Trial. J Clin Oncol. 2022;40(28):3246-56.

19. Turner N, Huang-Bartlett C, Kalinsky K, Cristofanilli M, Bianchini G, Chia S, et al. Design of SERENA-6, a phase III switching trial of camizestrant in *ESR1*-mutant breast cancer during first-line treatment. Future Oncol. 2023;19(8):559-73.

20. Araki K, Miyoshi Y. Mechanism of resistance to endocrine therapy in breast cancer: the important role of PI3K/Akt/mTOR in estrogen receptor-positive, HER2-negative breast cancer. Breast Cancer. 2018;25(4):392-401.

21. Cantley LC. The phosphoinositide 3-kinase pathway. Science. 2002;296(5573):1655-7.

22. O'Leary B, Hrebien S, Morden JP, Beaney M, Fribbens C, Huang X, et al. Early circulating tumor DNA dynamics and clonal selection with palbociclib and fulvestrant for breast cancer. Nat Commun. 2018;9(1):896.

23. Moynahan ME, Chen D, He W, Sung P, Samoila A, You D, et al. Correlation between *PIK3CA* mutations in cell-free DNA and everolimus efficacy in HR+, HER2- advanced breast cancer: results from BOLERO-2. Br J Cancer. 2017;116(6):726-30.

24. Board RE, Wardley AM, Dixon JM, Armstrong AC, Howell S, Renshaw L, et al. Detection of *PIK3CA* mutations in circulating free DNA in patients with breast cancer. Breast Cancer Res Treat. 2010;120(2):461-7.

25. Higgins MJ, Jelovac D, Barnathan E, Blair B, Slater S, Powers P, et al. Detection of tumor *PIK3CA* status in metastatic breast cancer using peripheral blood. Clin Cancer Res. 2012;18(12):3462-9.

26. Mollon LE, Anderson EJ, Dean JL, Warholak TL, Aizer A, Platt EA, et al. A Systematic Literature Review of the Prognostic and Predictive Value of PIK3CA Mutations in HR+/HER2- Metastatic Breast Cancer. Clin Breast Cancer. 2020;20(3):e232-e43.

27. André F, Ciruelos E, Rubovszky G, Campone M, Loibl S, Rugo HS, et al. Alpelisib for *PIK3CA*-Mutated, Hormone Receptor-Positive Advanced Breast Cancer. N Engl J Med. 2019;380(20):1929-40.

28. Baselga J, Im SA, Iwata H, Cortés J, De Laurentiis M, Jiang Z, et al. Buparlisib plus fulvestrant versus placebo plus fulvestrant in postmenopausal, hormone receptor-positive, HER2-negative, advanced breast cancer (BELLE-2): a randomised, double-blind, placebo-controlled, phase 3 trial. Lancet Oncol. 2017;18(7):904-16.

29. Miller TW, Hennessy BT, González-Angulo AM, Fox EM, Mills GB, Chen H, et al. Hyperactivation of phosphatidylinositol-3 kinase promotes escape from hormone dependence in estrogen receptor-positive human breast cancer. J Clin Invest. 2010;120(7):2406-13.

30. Miller TW, Balko JM, Fox EM, Ghazoui Z, Dunbier A, Anderson H, et al. ERα-dependent E2F transcription can mediate resistance to estrogen deprivation in human breast cancer. Cancer Discov. 2011;1(4):338-51.

31. Diehl F, Schmidt K, Choti MA, Romans K, Goodman S, Li M, et al. Circulating mutant DNA to assess tumor dynamics. Nat Med. 2008;14(9):985-90.

32. Diaz LA, Jr., Bardelli A. Liquid biopsies: genotyping circulating tumor DNA. J Clin Oncol. 2014;32(6):579-86.

33. Pascual J, Attard G, Bidard FC, Curigliano G, De Mattos-Arruda L, Diehn M, et al. ESMO recommendations on the use of circulating tumour DNA assays for patients with cancer: a report from the ESMO Precision Medicine Working Group. Ann Oncol. 2022;33(8):750-68.

34. NCCN Clinical Practice Guidelines in Oncology (NCCN Guidelines®) for Breast Cancer Version 2.2024. © National Comprehensive Cancer Network, Inc. 2024. All rights reserved. Accessed May 15, 2024.

35. Chiu J, Su F, Joshi M, Masuda N, Ishikawa T, Aruga T, et al. Potential value of ctDNA monitoring in metastatic HR + /HER2 - breast cancer: longitudinal ctDNA analysis in the phase Ib MONALEESASIA trial. BMC Med. 2023;21(1):306.

36. Bidard FC, Hardy-Bessard AC, Dalenc F, Bachelot T, Pierga JY, de la Motte Rouge T, et al. Switch to fulvestrant and palbociclib versus no switch in advanced breast cancer with rising *ESR1* mutation during aromatase inhibitor and palbociclib therapy (PADA-1): a randomised, open-label, multicentre, phase 3 trial. Lancet Oncol. 2022;23(11):1367-77.

37. Cardoso F, Paluch-Shimon S, Senkus E, Curigliano G, Aapro MS, André F, et al. 5th ESO-ESMO international consensus guidelines for advanced breast cancer (ABC 5). Ann Oncol. 2020;31(12):1623-49.

38. Takeshita T, Yamamoto Y, Yamamoto-Ibusuki M, Inao T, Sueta A, Fujiwara S, et al. Clinical significance of monitoring *ESR1* mutations in circulating cell-free DNA in estrogen receptor positive breast cancer patients. Oncotarget. 2016;7(22):32504-18.

39. Cabel L, Delaloge S, Hardy-Bessard A-C, Andre F, Bachelot T, Bieche I, et al. Dynamics and type of *ESR1* mutations under aromatase inhibitor or fulvestrant combined with palbociclib after randomization in the PADA-1 trial. In: Proceedings of the American Society of Clinical Oncology Annual Meeting; 2023 May 31; Chicago, IL. Abstract 1002. Available from: https://ascopubs.org/doi/10.1200/JCO.2023.41.16_suppl.1002

40. Hortobagyi GN, Chen D, Piccart M, Rugo HS, Burris HA, 3rd, Pritchard KI, et al. Correlative Analysis of Genetic Alterations and Everolimus Benefit in Hormone Receptor-Positive, Human Epidermal Growth Factor Receptor 2-Negative Advanced Breast Cancer: Results From BOLERO-2. J Clin Oncol. 2016;34(5):419-26.

41. Martínez-Sáez O, Chic N, Pascual T, Adamo B, Vidal M, González-Farré B, et al. Frequency and spectrum of *PIK3CA* somatic mutations in breast cancer. Breast Cancer Res. 2020;22(1):45.

42. Coombes RC, Page K, Salari R, Hastings RK, Armstrong A, Ahmed S, et al. Personalized Detection of Circulating Tumor DNA Antedates Breast Cancer Metastatic Recurrence. Clin Cancer Res. 2019;25(14):4255-63.

43. Velimirovic M, Juric D, Niemierko A, Spring L, Vidula N, Wander SA, et al. Rising Circulating Tumor DNA As a Molecular Biomarker of Early Disease Progression in Metastatic Breast Cancer. JCO Precis Oncol. 2020;4:1246-62.

44. Clatot F, Perdrix A, Beaussire L, Lequesne J, Lévy C, Emile G, et al. Risk of early progression according to circulating *ESR1* mutation, CA-15.3 and cfDNA increases under first-line anti-aromatase treatment in metastatic breast cancer. Breast Cancer Res. 2020;22(1):56.

45. Razavi P, Chang MT, Xu G, Bandlamudi C, Ross DS, Vasan N, et al. The Genomic Landscape of Endocrine-Resistant Advanced Breast Cancers. Cancer Cell. 2018;34(3):427-38.e6.

46. Shibayama T, Low SK, Ono M, Kobayashi T, Kobayashi K, Fukada I, et al. Clinical significance of gene mutation in ctDNA analysis for hormone receptor-positive metastatic breast cancer. Breast Cancer Res Treat. 2020;180(2):331-41.

47. Takeshita T, Yamamoto Y, Yamamoto-Ibusuki M, Tomiguchi M, Sueta A, Murakami K, et al. Analysis of *ESR1* and *PIK3CA* mutations in plasma cell-free DNA from ER-positive breast cancer patients. Oncotarget. 2017;8(32):52142-55.

48. Johnston SR, Kilburn LS, Ellis P, Dodwell D, Cameron D, Hayward L, et al. Fulvestrant plus anastrozole or placebo versus exemestane alone after progression on non-steroidal aromatase inhibitors in postmenopausal patients with hormone-receptor-positive locally advanced or metastatic breast cancer (SoFEA): a composite, multicentre, phase 3 randomised trial. Lancet Oncol. 2013;14(10):989-98.

49. Bardia A, Su F, Solovieff N, Im SA, Sohn J, Lee KS, et al. Genomic Profiling of Premenopausal HR+ and HER2- Metastatic Breast Cancer by Circulating Tumor DNA and Association of Genetic Alterations With Therapeutic Response to Endocrine Therapy and Ribociclib. JCO Precis Oncol. 2021;5.

50. Park YH, Im SA, Park K, Wen J, Lee KH, Choi YL, et al. Longitudinal multi-omics study of palbociclib resistance in HR-positive/HER2-negative metastatic breast cancer. Genome Med. 2023;15(1):55.

51. Haber DA, Velculescu VE. Blood-based analyses of cancer: circulating tumor cells and circulating tumor DNA. Cancer Discov. 2014;4(6):650-61.

52. Hindson BJ, Ness KD, Masquelier DA, Belgrader P, Heredia NJ, Makarewicz AJ, et al. High-throughput droplet digital PCR system for absolute quantitation of DNA copy number. Anal Chem. 2011;83(22):8604-10.

53. Forshew T, Murtaza M, Parkinson C, Gale D, Tsui DWY, Kaper F, et al. Noninvasive identification and monitoring of cancer mutations by targeted deep sequencing of plasma DNA. Sci Transl Med. 2012;4(136):136ra68.

54. Sim SH, Yang HN, Jeon SY, Lee KS, Park IH. Mutation analysis using cell-free DNA for endocrine therapy in patients with HR+ metastatic breast cancer. Sci Rep. 2021;11(1):5566.

55. Sathe C, Accordino MK, DeStephano D, Shah M, Wright JD, Hershman DL. Social determinants of health and CDK4/6 inhibitor use and outcomes among patients with metastatic breast cancer. Breast Cancer Res Treat. 2023;200(1):85-92.

국문요약

배경: *ESR1* 및 *PIK3CA* 유전자의 활성화 돌연변이는 내분비 저항성의 기전으로 알려져 있다. 최근 연구들은 임상적으로 질병이 진행되기 전, 혈액 내 *ESR1* 돌연변이(b*ESR1*)가 존재할 때 조기 개입의 이점을 보여주었다. 이 연구에서는 호르몬 수용체 양성, 인간 상피 성장 인자 수용체 2 음성 전이성 유방암 환자의 세포유리 DNA 에서 *ESR1* 및 *PIK3CA* 돌연변이의 검출과 변화, 그리고 이 돌연변이들이 무진행 생존 기간에 미치는 영향을 조사하고자 하였다.

방법: 1 차 완화적 내분비 요법을 받고 있는 25 명의 환자가 전향적 코호트에서 확인되었다. 리간드 결합 도메인의 7 개 *ESR1* 호발 부위 돌연변이를 미세방울 디지털 중합효소연쇄반응 분석을 사용하여 세포유리 DNA 에서 검사했다. 11 개의 *PIK3CA* 호발부위 돌연변이는 종양과 세포유리 DNA 모두에서 앰플리콘 기반 표적 차세대 시퀀싱 방법을 사용하여 검사했다. 무진행 생존 기간 분석은 카플란-마이어 생존 분석 방법을 사용하여 수행되었으며 로그 순위법으로 비교되었다.

결과: 본 연구에서는 25 명의 환자로부터 약 3~6 개월마다 수집된 일련의 세포유리 DNA 샘플 268 개를 분석했다. b*ESR1* 은 완화적 내분비 요법 동안 64.0%(16/25)의 환자에서 발견되었으며, D538G 가 가장 흔한 돌연변이였고 68.8%는 다클론성이었다. b*ESR1* 이 검출된 환자 중 임상적으로 질병 진행이 있는 경우는 50.0%였는데, 이 중 4 명은 임상적 질병 진행 전에 b*ESR1* 이 검출되었고, 4 명은 질병 진행과 동시에 또는 이후에 검출되었다. b*ESR1* 은 전체 무진행 생존기간에 영향을 미치지 않았지만, 1 차 내분비 치료 후 6 개월 이내에 b*ESR1* 이 검출된 환자 (18.8%)는 더 나쁜 생존 결과를 보였다 (무진행 생존 기간 중앙값 5.5 대 53.6 개월). 또한 후속 세포유리 DNA 에서 b*ESR1* 이 소실된 환자(81.3%)는 더 나은 결과를 보이는 것으로 나타났다 (무진행 생존 기간

중앙값 53.6 개월 대 42.4 개월). 세포유리 DNA 에서 *PIK3CA* 돌연변이는 원격 전이 진단 시 68.2%(15/22)의 환자에서 발견되었으며, 그 중 53.3%(8/15)의 환자에서 b*ESR1*이 발견되었다. 원발 종양 조직에서 *PIK3CA* 돌연변이의 존재는 무병 생존 기간이나 무진행 생존 기간에 영향을 미치지 않았지만, 혈액 *PIK3CA* 돌연변이가 있는 환자는 무진행 생존 기간이 유의하게 더 나빴다 (p = 0.024).

결론: 이 연구에서는 상당한 수의 *ESR1* 및 *PIK3CA* 돌연변이가 일련의 혈장에서 검출되었다. 통계적 유의성을 정확하게 평가하기에는 한계가 있는 소규모 분석이었지만, 완화적 내분비 치료 시작 6 개월 이내 b*ESR1*이 조기 검출된 경우와 지속 검출된 환자의 경우 더 나쁜 결과를 보였다. 세포유리 DNA 에서 *PIK3CA* 돌연변이는 표적 치료의 이점을 시사하는 예후 인자였다.